AD-A171 360 KINETICS AND MECHANISMS ON THE MOLECULAR BEAM ETCHING OF SEMICONDUCTORS(U) HUGHES RESEARCH LABS MALIBU CA H P GILLIS JUL 86 ARO-19868.1-EL DAAG29-82-C-0020 1/1

UNCLASSIFIED F/G 13/8 NL

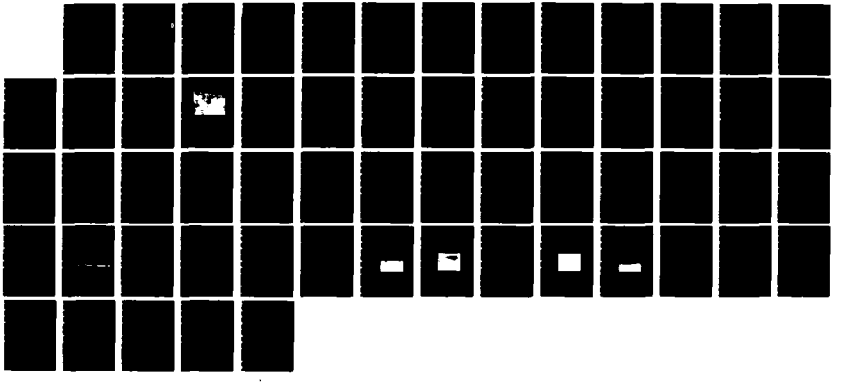

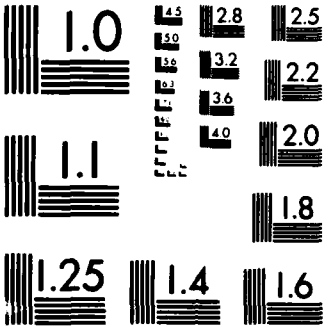

KINETICS AND MECHANISMS IN THE MOLECULAR BEAM ETCHING OF SEMICONDUCTORS

H.P. Gillis

Hughes Research Laboratories
3011 Malibu Canyon Road
Malibu, CA 90265

July 1986

DAAG29-82-C0020
Final Report
15 August 1982 through 15 February 1986

U.S. Army Research Office
Post Office Box 12211
Research Triangle Park, NC 27709

REPORT DOCUMENTATION PAGE

1a. REPORT SECURITY CLASSIFICATION Unclassified	1b. RESTRICTIVE MARKINGS
2a. SECURITY CLASSIFICATION AUTHORITY	3. DISTRIBUTION/AVAILABILITY OF REPORT Unlimited
2b. DECLASSIFICATION/DOWNGRADING SCHEDULE	
4. PERFORMING ORGANIZATION REPORT NUMBER(S)	5. MONITORING ORGANIZATION REPORT NUMBER(S) ARO 19068.1-EL
6a. NAME OF PERFORMING ORGANIZATION Hughes Research Laboratories 6b. OFFICE SYMBOL (If applicable)	7a. NAME OF MONITORING ORGANIZATION
6c. ADDRESS (City, State and ZIP Code) 3011 Malibu Canyon Road Malibu, CA 90265	7b. ADDRESS (City, State and ZIP Code)
8a. NAME OF FUNDING/SPONSORING ORGANIZATION U.S. Army Research Office 8b. OFFICE SYMBOL (If applicable)	9. PROCUREMENT INSTRUMENT IDENTIFICATION NUMBER DAAG29-82-C0020
8c. ADDRESS (City, State and ZIP Code) Post Office Box 12211 Research Triangle Park, NC 27709	10. SOURCE OF FUNDING NOS. PROGRAM ELEMENT NO. / PROJECT NO. / TASK NO / WORK UNIT NO.
11. TITLE (Include Security Classification) Kinetics and Mechanisms in the Molecular Beam Etching of Semiconductors	
12. PERSONAL AUTHOR(S) H.P. Gillis	
13a. TYPE OF REPORT Final Report 13b. TIME COVERED FROM 15/8/82 TO 15/2/86	14. DATE OF REPORT (Yr., Mo., Day) July 1986 15. PAGE COUNT
16. SUPPLEMENTARY NOTATION	
17. COSATI CODES FIELD / GROUP / SUB GR	18. SUBJECT TERMS (Continue on reverse if necessary and identify by block number) Molecular beam etching (MOBE), ion-beam assised etching (IBAE), reactive ion beam etching (RIBE), selectivity,

19. ABSTRACT (Continue on reverse if necessary and identify by block number)

The main issue addressed was the role of the ion beam in control of anisotropy and selectivity in the ion-beam assisted etching (IBAE) of layered samples of Si and SiO_2, as are used in CMOS gate applications. The results on patterned samples were correlated directly with the geometrical relationship of the incident beams and the sample. Rate dat were obtained which suggest that the reaction proceeds by facilitated attack of reactant species at defect sites created by the ion beam. It was demonstrated that ion beam energy greater than 500 eV caused inadequate selectivity between Si and SiO_2. It was shown that inadequate selectivity is the main problem holding back implementation of IBAE as a practical process. It is suggested that additional work in the direction of low-energy IBAE (50-500 eV) be pursued.

20. DISTRIBUTION/AVAILABILITY OF ABSTRACT UNCLASSIFIED/UNLIMITED ☒ SAME AS RPT ☐ DTIC USERS ☐	21. ABSTRACT SECURITY CLASSIFICATION
22a. NAME OF RESPONSIBLE INDIVIDUAL H.P. Gillis	22b TELEPHONE NUMBER (Include Area Code) (213)317-5576 22c. OFFICE SYMBOL

18. SUBJECT TERMS (Continued)
anisotropy, time-resolved laser reflectivity (TRR), radiation damage, low-energy ion beams.

FOREWORD

This is the Final Report summarizing work performed at Hughes Research Laboratories under Contract No. DAAG29-82-C0020 (Kinetics and Mechanisms in the Molecular Beam Etching of Semiconductors) with the Army Research Office. H.P. Gillis was Principal Investigator and is author of this report.

The main issue addressed was the role of the ion beam in control of anisotropy and selectivity in the ion-beam assisted etching (IBAE) of layered samples of Si and SiO_2, as are used in CMOS gate applications. The results on patterned samples were correlated directly with the geometrical relationship of the incident beams and the sample. Rate data were obtained which suggest that the reaction proceeds by facilitated attack of reactant species at defect sites created by the ion beam. It was demonstrated that ion beam energy greater than 500 eV caused inadequate selectivity between Si and SiO_2. It was shown that inadequate selectivity is the main problem holding back implementation of IBAE as a practical process. It is suggested that additional work in the direction of low-energy IBAE (50-500 eV) be pursued.

The author is indebted to L.J. Miller and F.G. Yamagishi for their assistance in the formulation and planning of the program. He is indebted to G.L. Olson for numerous, helpful discussions on laser reflectivity and to R.L. Poeschel and J.W. Ward for numerous, helpful discussions on operation of ion sources. He is indebted to A.R. Ward and the late C.P. Hoberg for expert technical assistance. He is especially indebted to his colleague W.J. Gignac for writing the computer code to calculate reflectivity of layered samples, for computerizing the acquisition of reflectivity data, for designing and constructing the ion beam imaging unit and the retarding field analyzer, and for collecting most of the experimental data reported here.

TABLE OF CONTENTS

LIST OF ILLUSTRATIONS

SECTION 1

INTRODUCTION AND BACKGROUND

During the last decade it has been recognized that plasma-assisted dry etching is necessary for fabrication of microelectronic devices from patterns having sub-micrometer features. Development of practical processes has been carried out empirically in plasma reactors where halogen-bearing molecules are fragmented by the glow discharge into reactive ions and radicals which react with the substrate to produce volatile species.[1] In order to simulate the complicated chemistry in the discharge under more controlled conditions, Coburn and Winters introduced the method of Ion Beam Assisted Etching (IBAE) in which independent beams of inert ions and reactive molecules are simultaneously applied to the substrate.[2] They demonstrated that the two beams have a synergistic effect on the etching rate and have since used their method to obtain substantial insight into the nature of the etching reactions.[3]

In 1981, we undertook research at Hughes Research Laboratories (HRL) to see whether the IBAE approach could form the basis for a new processing method which would remove some of the shortcomings of plasma reactors. We felt that the independent control of the ionic and reactive species available in the beam method, along with *in situ* process monitors, would enable processes to be developed more quickly and systematically than in the plasma reactors. Moreover, the independent control of species should enable processes developed in one beam system to be implemented readily in another beam system. (Transfer of processes between plasma systems has proved notoriously difficult because not all reaction conditions at the substrate are under direct control of the experimenter.)

In 1982, this program at HRL was supplemented by Contract No. DAAG29-82-C-0020, "Kinetics and Mechanisms in the Molecular Beam Etching of Semiconductors," from the Army Research Office.

In this Final Report we summarize our progress and identify the problems which remain to be solved before the beam approach can be made into a practical process method.

A. PROBLEM

The key issue in development of dry etching processes is very careful control and manipulation of the *relative* rates of chemical reactions at the substrate (see Figure 1). The relative reaction rate of two different solids in a layered structure exposed to given reaction conditions must be large enough to achieve selectivity. This is especially important in device designs which require substantial over-etching. In a single layer, the rate in the vertical direction must greatly exceed that in the lateral plane to achieve anisotropy.

It is generally recognized that in plasma etchers, anisotropy relies upon bombardment of the substrate by ions. (See Figure 2.) It is not yet understood whether this is due solely to normal incidence of the ions, or whether some passivation of the sidewalls by involatile side products of the etching reaction (e.g., polymeric films from Freon-type etchants) is required as well.[1] Isotropic etching, or under-cutting, is attributed to the diffusion of reactive species with short mean-free path lengths through the pattern opening. Selectivity is obtained in plasma etchers by using mixtures of gases. For example, adding H_2 to a CF_4 discharge scavenges the F atoms and leaves a relative abundance of CF_3 radicals which passivate Si surfaces with carbon but which readily etch SiO_2 because the oxygen in the film reacts with the carbon to prevent build-up. The basic premise in plasma-assisted etching is, therefore, that anisotropy traces to ion-surface interactions and selectivity to the identity and concentration of reactive radical species.

Although numerous successful plasma etching processes have been developed, certain general problems remain.[1] In general, there is not independent control of the ionic and radical species, so that compromises between anisotropy and selectivity

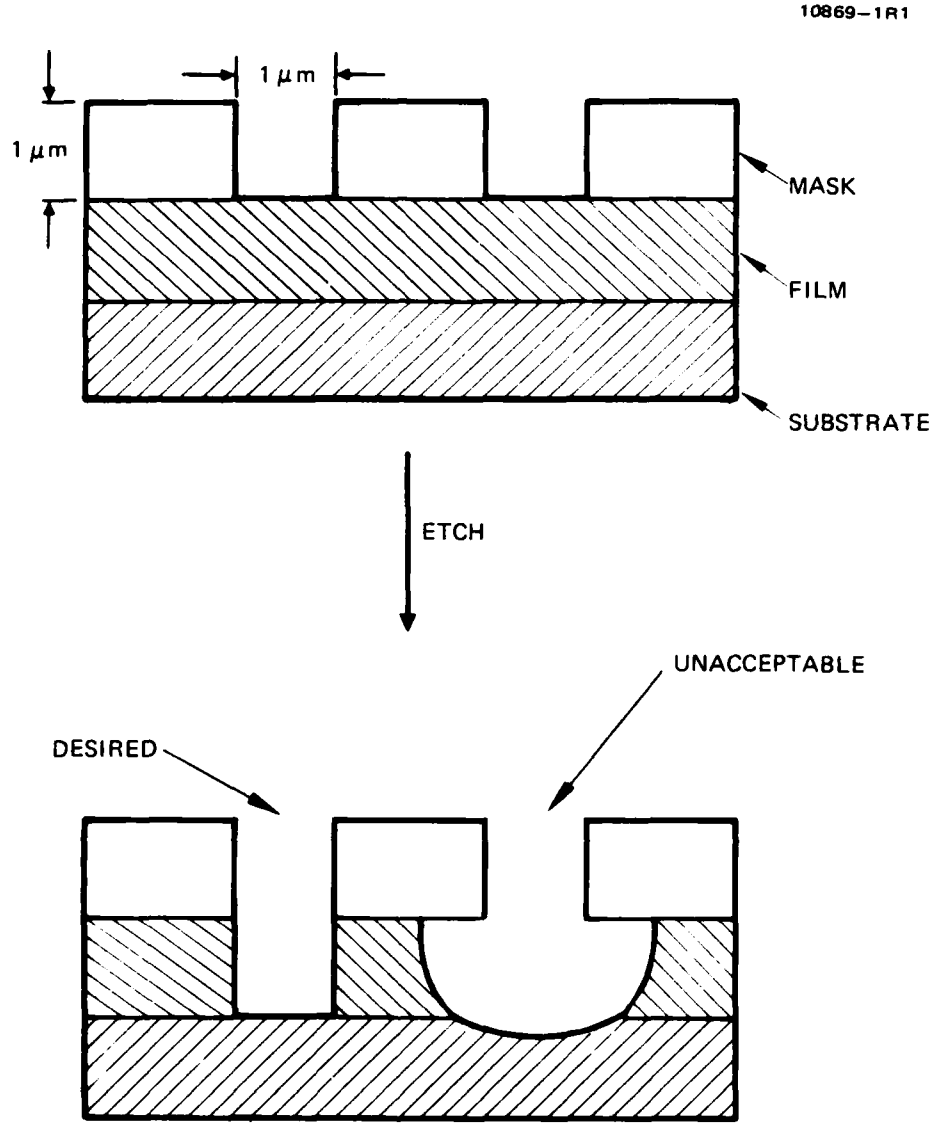

Figure 1. A typical etching assignment. The etch must show preference, i.e., selectivity, for the film; extensive overetching into the substrate will weaken and perhaps destroy the device. Moreover, the etch must be faster in the vertical than in the lateral direction, i.e., it must be anisotropic; otherwise, substantial undercutting will occur, and the dimensional integrity of the device will be compromised. Finally, the etch must be sufficiently fast to enable device production with acceptable throughput.

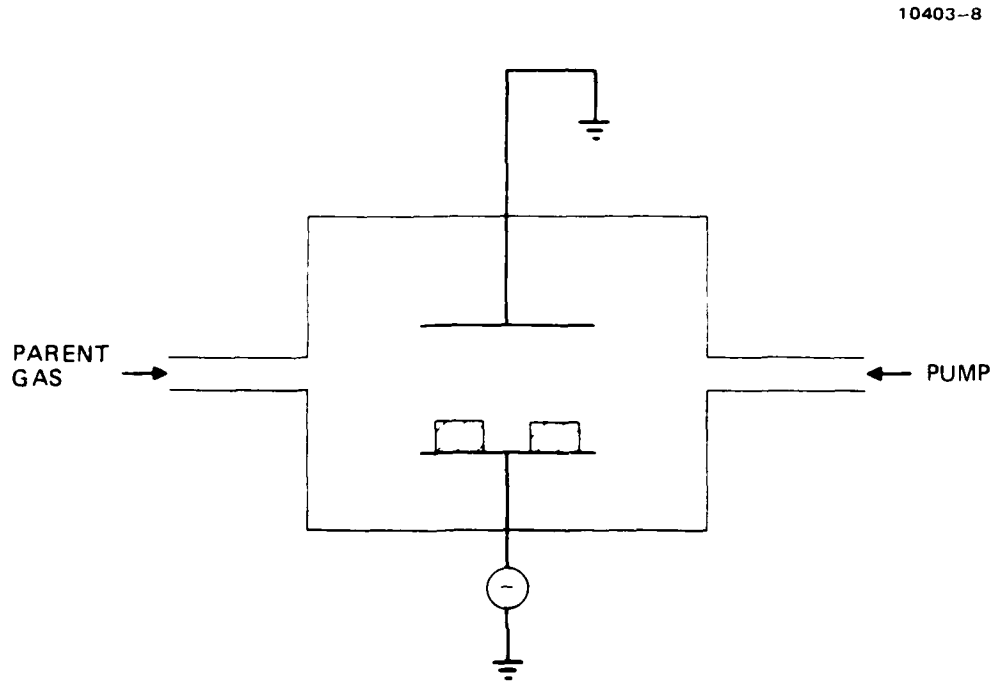

Figure 2. Plasma reactor in the planar configuration. Wafers sit on the powered electrode. The discharge between electrodes dissociates the parent gas into radicals and ions. The radicals diffuse to the wafer; the ions are accelerated by the potential difference between the body of plasma and the powered electrode.

are difficult to work out. There are high-energy tails on the ion energy distribution,[4] and these can cause substrate damage during processing.[5] Complex etching mixtures, especially those containing Freon-type molecules, can leave residues and deposits (e.g., silicon carbide) which can affect electrical properties and interfere with subsequent process steps.[6] Because the sample is immersed in plasma, products of the reaction are subject to numerous secondary reactions and kinetic analysis of the reactions is difficult.

The IBAE approach offers the potential to solve these problems in process development. The specific problem which was addressed in this program is the following: can good anisotropy and selectivity be obtained in polycrystalline silicon films over SiO_2 by using IBAE with an Ar^+ ion beam and a Cl_2 molecular beam? The applied objective was to identify reaction conditions which would enable a process to be developed with very simple chemistry and with no reliance upon additives which would passivate or leave residues. The fundamental objective was to elucidate the role of the ion beam in "assisting" the etch chemistry and to see whether the ion beam, which is essential for anisotropy, can compromise selectivity.

B. APPROACH

Our approach to this problem can be summarized by returning to Figure 1. We take the point of view that in IBAE anisotropy can be produced by properly directed beams of ions and reactive molecules. By maintaining background pressure of 10^{-5} -10^{-6} Torr during the reaction, we can minimize diffusion of reactive species to the substrate and expect thereby to minimize undercutting. We view the issue of selectivity as being somewhat analogous to depth profiling of layered samples by SIMS; the difference is that in etching we want to measure changes in reactivity rather than in composition at an interface. We accomplish this by simultaneous application of mass spectrometry (MS) and of time-resolved laser reflectivity (TRR). By using TRR

as a "depth index" in a layered sample, we can identify etch products with MS as a function of depth and thereby relate changes of reactivity at the interface to etching conditions. Thus our approach includes these features:

- simple chemistry
- geometrical control of incident species for anisotropy
- narrow ion energy distribution
- variable ion energy and current density
- *in situ* reaction monitors

Our general procedure is to vary the ionic and reactive fluxes and use the reaction monitors to identify conditions which enable good anisotropy and selectivity for poly Si and SiO_2. In the early stages of the program we used NF_3 as the reactant gas. However we obtained better selectivity with Cl_2 and used it for the majority of the work.

Our laboratory system is shown schematically in end view in Figure 3. We have named it the Molecular Beam Etching (MOBE) System since it affords the flexibility to study several beam-based methods of etching, including Ion Beam Assisted Etching (IBAE) and Reactive Ion Beam Etching (RIBE). The chamber is a stainless steel cylinder, 14 in. in diameter, with its axis placed horizontal in the lab. The system is evacuated by a turbomolecular pump with 2000 liters/sec pumping speed. Base pressure of the system is $1x10^{-8}$ Torr. The ion source is of the Kaufman type, with the standard multi-apertured, two-grid extraction optics.[7] The accelerator grid is 6 in. from the sample. A blocking plate of stainless steel (held at earth potential) is interposed between accelerator and sample; a circular aperture in it admits a circular ion beam spot about 1 cm in diameter at the sample. The reactive gas is delivered by a quartz tube with an aperture 1 mm in diameter at the end. The reactive flux to the sample can be calculated by the standard methods.[8] The sample can be rotated about an axis perpendicular to the plane of the paper in order to vary the angle of incidence

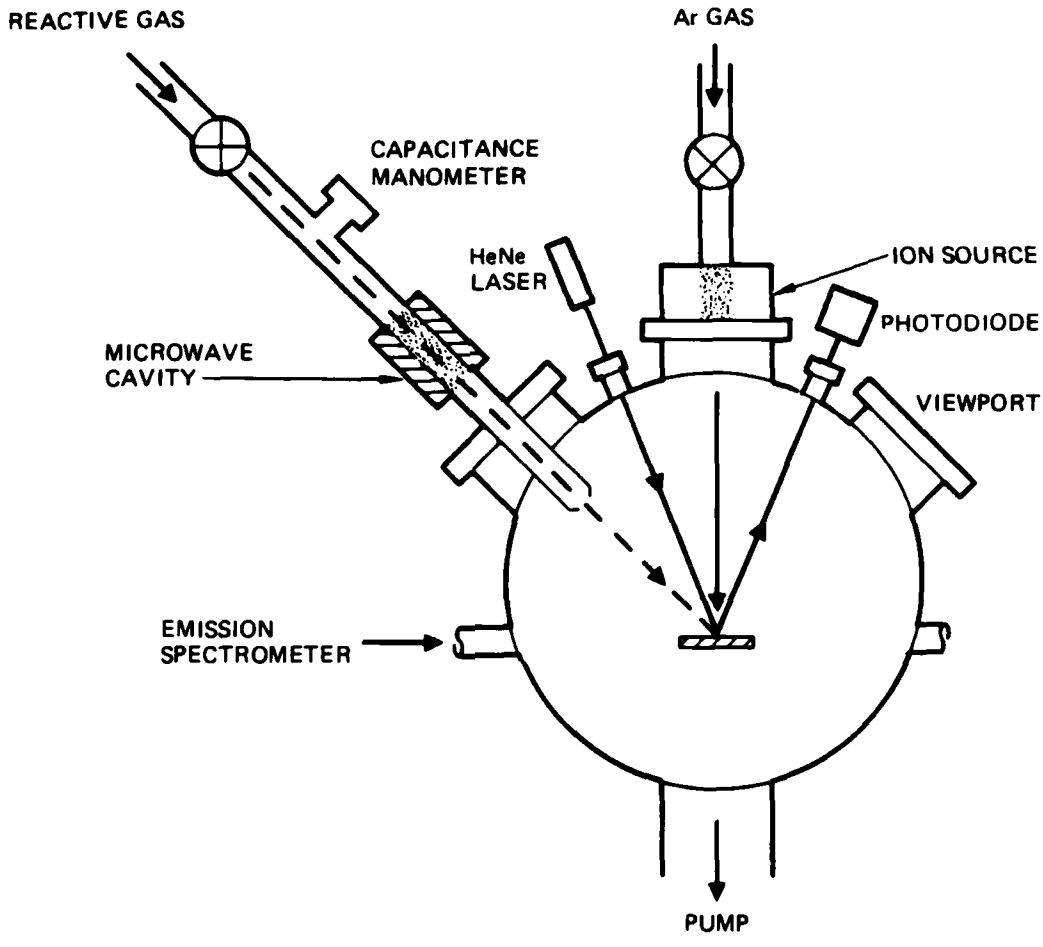

Figure 3. Schematic of the reaction chamber in the MOBE system at HRL. Ion and radical beams are applied simultaneously to achieve both anisotropy and high etch rate. The sample can be rotated about an axis perpendicular to the paper in order to vary the angle of incidence for each of the beams. The microwave cavity and emission spectrometer were not used in the work reported here.

for each of the beams. A photograph of the system from the same point of view is shown in Figure 4. A He-Ne laser and photodiode detector are used for TRR. The MS with cross-beam ionizer is mounted in a flight tube which observes the sample at an angle 45° below the normal and has two stages of differential pumping. The installation is shown schematically in side view in Figure 5. Similar MS installations have been used by others in IBAE.[3,9]

Our experimental procedure consists of varying the ion beam energy and current (for a given Cl_2 flux), measuring the etch rate and depth by TRR, and identifying products by MS. Thus we obtain *in situ* a direct measurement of selectivity (from TRR) as well as some insight into the chemical reactions involved (from MS) for each set of etching conditions.

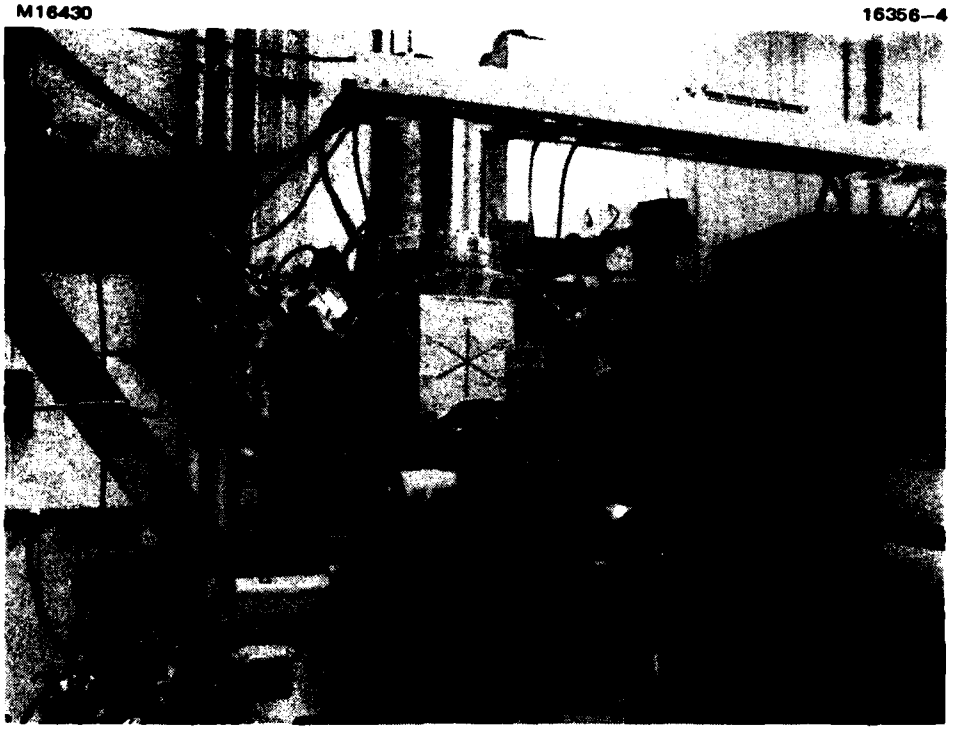

Figure 4. Photograph of MOBE system.

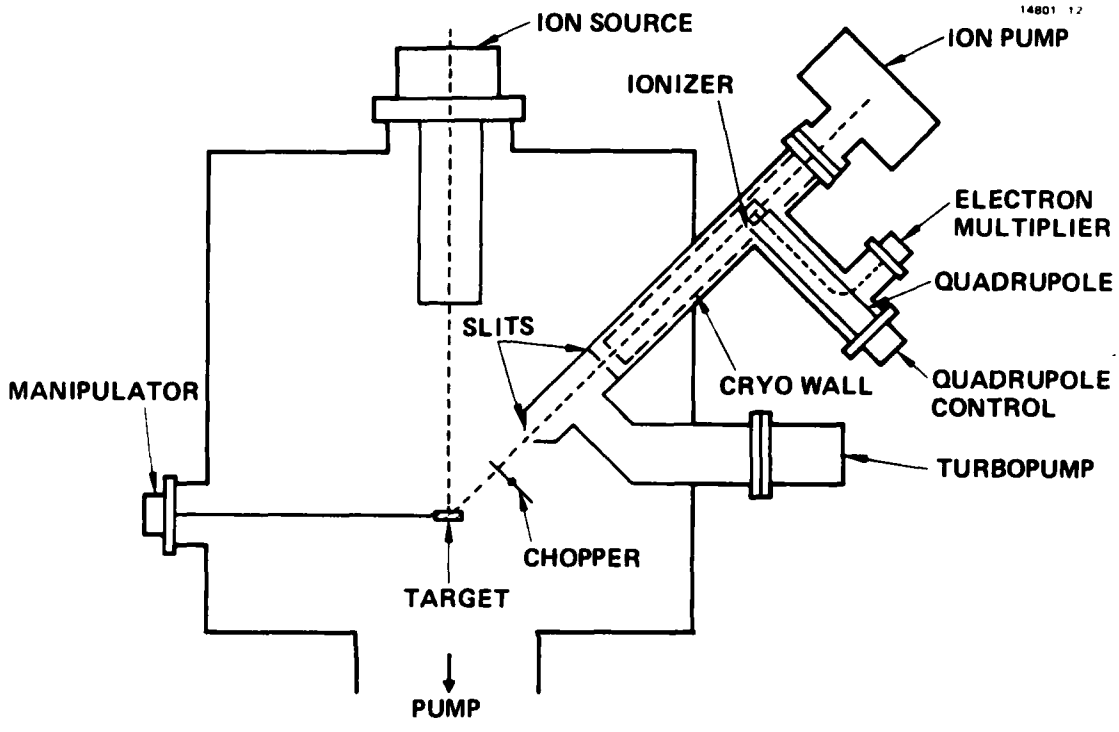

Figure 5. MOBE MS installation. The MS unit has two stages of differential pumping. Typical operating conditions have 10^{-5} Torr in the main chamber, 10^{-7} Torr in the first stage, 10^{-9} Torr at the ionizer.

SECTION 2

EXPERIMENTAL RESULTS

This program has been organized as a search for conditions which permit good anisotropy and selectivity between poly Si and SiO_2 using simple chemistry and *in situ* monitors in IBAE. The results are presented here as six steps toward that goal. They are as follows: (a) development of time-resolved laser reflectivity (TRR) as a process monitor; (b) characterization of the current and energy distribution from the Kaufman ion source; (c) measurements of reaction rates; (d) results obtained by MS; (e) formulation of a reaction model for selectivity; (f) results for patterned samples.

A. TIME-RESOLVED LASER REFLECTIVITY

It is highly desirable to measure the etch rate directly at the surface and not rely solely upon detection of volatile products. It is also desirable to obtain reaction data resolved in both time and depth. The method of time resolved laser reflectivity (TRR) has been developed in a form to provide these capabilities in the solid-phase epitaxy research programs at HRL.[10] The method is very generally applicable to measuring the change in thickness of a thin film (between two other materials having different indices of refraction) induced during a given process. Indeed, the method has already been applied by others to determine end point and average etch rate in conventional plasma etching.[11] We have developed methods for extracting more information from the reflectivity data, including rate as a function of time and depth.

The principles behind the application of TRR to measurement of etch rate are summarized in Figure 6. Our procedure comprises three steps: (1) provision *a priori* of the reflectivity of the sample to be etched as a function of film thickness, as in Figure 6(C); (2) measurement of the real-time reflectivity of the sample during etching, as in Figure 6(B); and (3) processing of

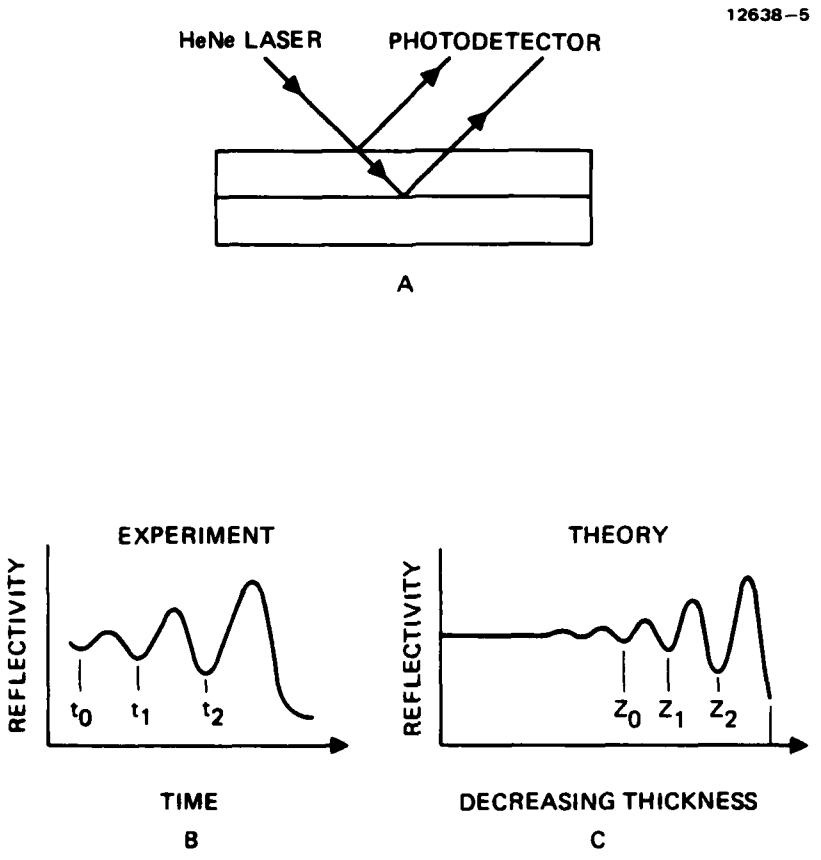

Figure 6. The method of time-resolved laser reflectivity (TRR) for measurement of etch rate. Laser light incident upon the layered sample is partly reflected at the vacuum interface and partly at the material interface. These two reflected beams interfere, and the total reflected intensity arrives at the photodetector (A). Because the light is monochromatic, the total reflectivity goes through oscillations as the top layer is removed. The initial value is characteristic of the top layer, the final asymptotic value is characteristic of the second layer (B). With a theoretical expression for reflectivity of the upper layer as a function of thickness (C), the experimental data (B) can be inverted to give instantaneous etch depth. The instantaneous etch rate follows by differentiation.

the experimental data to obtain average etch rate, instantaneous etch rate, or etch rate as a function of depth.

We obtain the *a priori* reflectivity R as a function of film thickness z by a computer simulation based on Equation (1).[10] For a plane wave normally incident on the film (film index n_1, substrate index n_2) the reflectivity (R) can be expressed as a function of the film thickness:

$$R = \left[\frac{\rho_{01} + \rho_{12} e^{-\alpha z} e^{-i2kz}}{1 + \rho_{01}\rho_{12} e^{-\alpha z} e^{-i2kz}}\right]^2 , \qquad (1)$$

where ρ_{01} and ρ_{12} are the reflection coefficients at the vacuum/film and film/substrates interfaces, respectively.

and

$$\rho_{01} = (1 - n_1)/(1 + n_1)$$
$$\rho_{12} = (n_1 - n_2)/(n_1 + n_2) ,$$

and α and k are the absorption coefficient and wavenumber of the incident light in the film. Thus

$$\alpha \equiv \frac{4\pi}{\lambda} \mathrm{Im}(n_1)$$

$$k \equiv \frac{2\pi}{\lambda} \mathrm{Re}(n_1) .$$

We have written a Fortran program which calculates R for a sample with as many as ten layers. The required input data are the thickness and complex index of refraction for each layer. We have applied this method to samples of amorphous Si over crystalline Si (prepared by double implantation of $^{28}Si^+$ at 120 keV and 70 keV into Si(100)). This is a good test case because the TRR behavior is already understood from the recrystallization work at HRL. It is also a meaningful case study for etching since the ion beam in IBAE will render amorphous a crystalline substrate. As an example, we show in Figure 7 calculated reflectivity for

film of 4000 Å of a-Si over crystalline Si (refractive index 4.85-i0.612 and 4.16-i0.018, respectively, and wavelength λ=6328 Å for He-Ne laser light). The horizontal axis measures the amount of a-Si *removed* from the film initially 4000 Å thick, so film thickness *decreases* toward the right in this figure. The amplitude of the modulation in reflectivity increases as the film is thinned because a-Si absorbs He-Ne light, and it asymptotically approaches the value for crystalline Si. In Figure 8 we show a direct comparison of computer simulation and experimental measurement of the reflectivity for etching away a film of 3600 Å of a-Si from a substrate of crystalline Si. This demonstrates that our simulation produces physically correct results.

Rate information is obtained as follows. Since constructive interference between waves occurs at every half-wavelength of light in the medium, each peak in Figure 7 is separated from the adjacent peaks by $\lambda/2n$. For a-Si and He-Ne light, this corresponds to removal of an incremental thickness Δz = 652 Å. On the experimental trace (obtained with a strip chart recorder) in Figure 8, the same separation of peaks is accomplished in a time interval Δt. Therefore, the measured etch rate is defined as $r = \Delta z/\Delta t$. Thus, with a simple analog system we can measure the average etch rate in each 650 Å of a-Si removed, which enables etch rate to be determined as a function of depth. For example, we always see the etch rate start out somewhat slowly and then increase as a thin layer of surface oxide is removed. It is possible to digitize the experimental signal and have the computer perform the comparison with the simulation in order to obtain the etch rate as a *continuous* function of depth. We have not yet put this feature into practice.

In Figure 9, we illustrate the capability of TRR to give real-time, *in situ* measurements of etch rate as a function of etch conditions. We compare the results for etching two samples of 3600 Å of a-Si over Si. The first sample was milled with a beam of Ar^+ ions. The second was exposed to identical ion beam conditions simultaneous with a beam of Cl_2 molecules. Addition

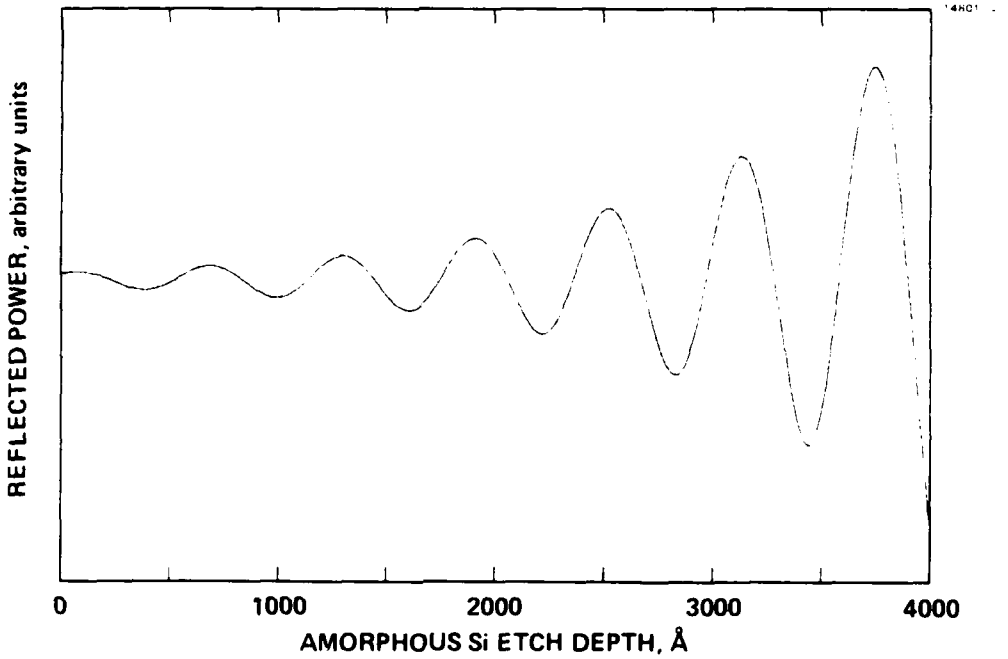

Figure 7. Computer simulation of TRR data for etching of a-Si on Si.

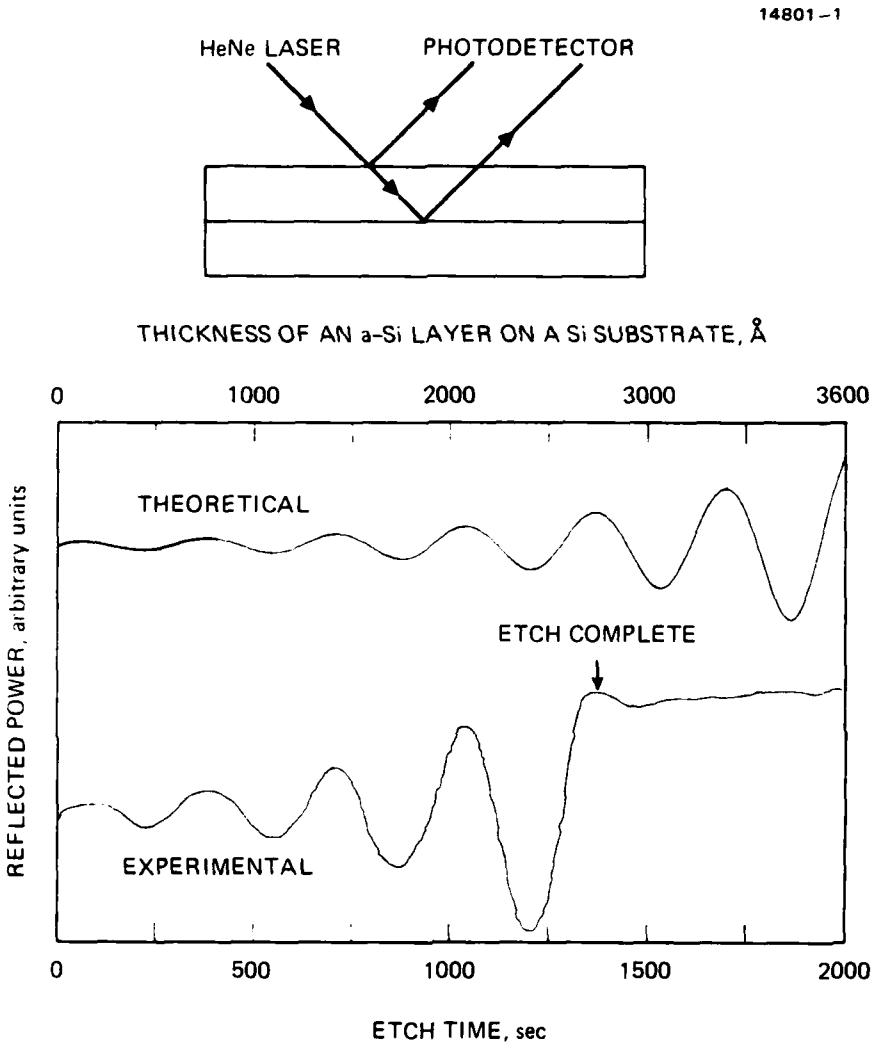

Figure 8. Basics of time resolved reflectivity (TRR). Extra path length gives interference as upper layer is removed. Comparison of experimental data and theoretical simulation gives rate data.

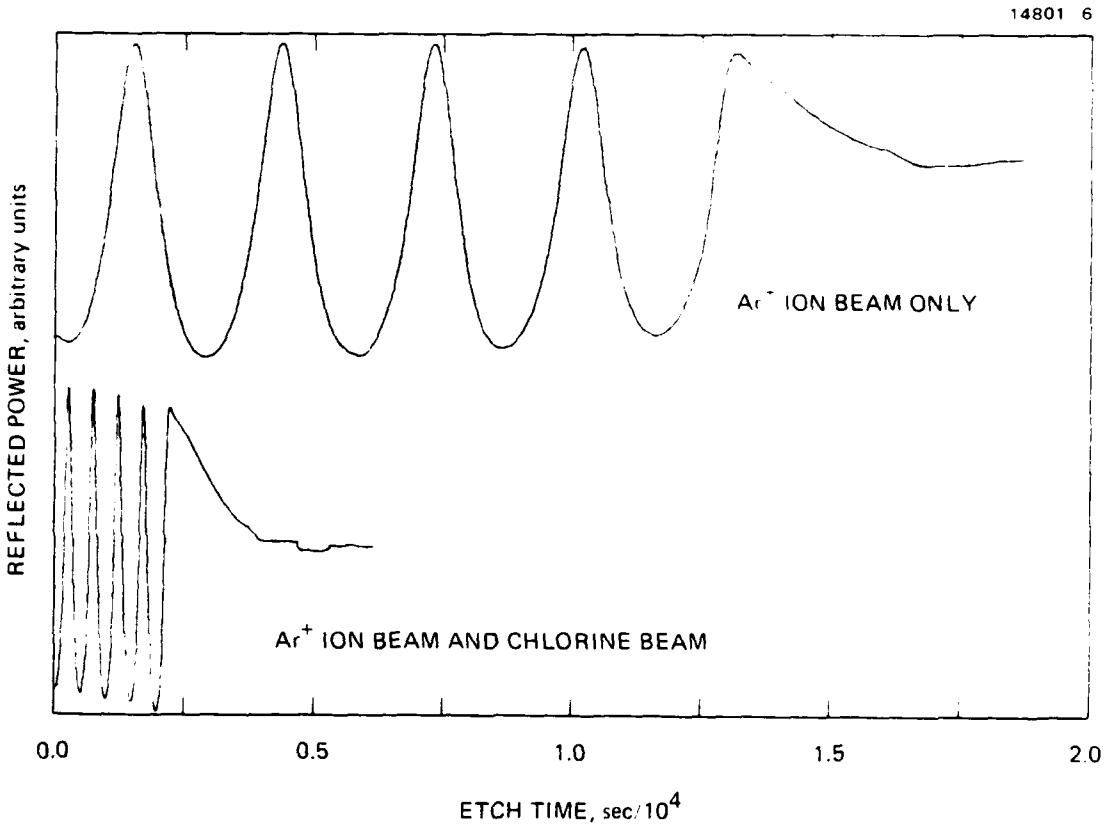

Figure 9. Experimental TRR data for etching of a-Si on Si. The rate increases by about a factor of 6 when the chlorine beam is added to the ion beam.

of the Cl_2 increased the etch rate by about a factor of 6. Since Cl_2 does not react with Si at room temperature, this experiment illustrates and confirms the synergistic effect of the two beams which Coburn and Winters named "ion-assisted etching."[2]

This simple example shows the power and utility of TRR as a real-time, *in situ* probe of etching reaction rates. We have used TRR in this way throughout the program to relate etch rate to reaction conditions. We give one additional example here to show that for a three-layer sample (e.g., poly Si over SiO_2 over crystalline Si) TRR gives an immediate measurement of selectivity. In Figure 10, we show the computer simulation of the reflectivity to be expected as we etch through a sample comprising 4000 Å of poly Si over 1000 Å of SiO_2 over bulk Si. In Figure 11, we show experimental TRR data for etching two such samples. The first one was milled by Ar^+ ions; the second saw identical ion beam conditions and also a Cl_2 molecular beam. Again we see the synergistic effect of ion enhancement. In addition, we can see that with both beams present, poly Si etched about 3 times as fast as SiO_2 for a selectivity of 3:1. This real-time measurement of selectivity is very valuable since, in conventional techniques, it is necessary to remove the sample from the etcher, fracture it, examine the edge in SEM, and estimate the relative amount of film removed from the two layers. Moreover, we will show in a subsequent Section that simultaneous application of TRR with MS enables identification of volatile etch products as a function of depth, as well as giving the types of rate information already illustrated here.

A similar development of computer simulation of the TRR signal was in progress at Bell Laboratories at the same time as our work.[1]

B. CHARACTERIZATION OF KAUFMAN ION SOURCE

In order to expose the effects of the ion beam upon the etching reaction, it is necessary to measure the current density and

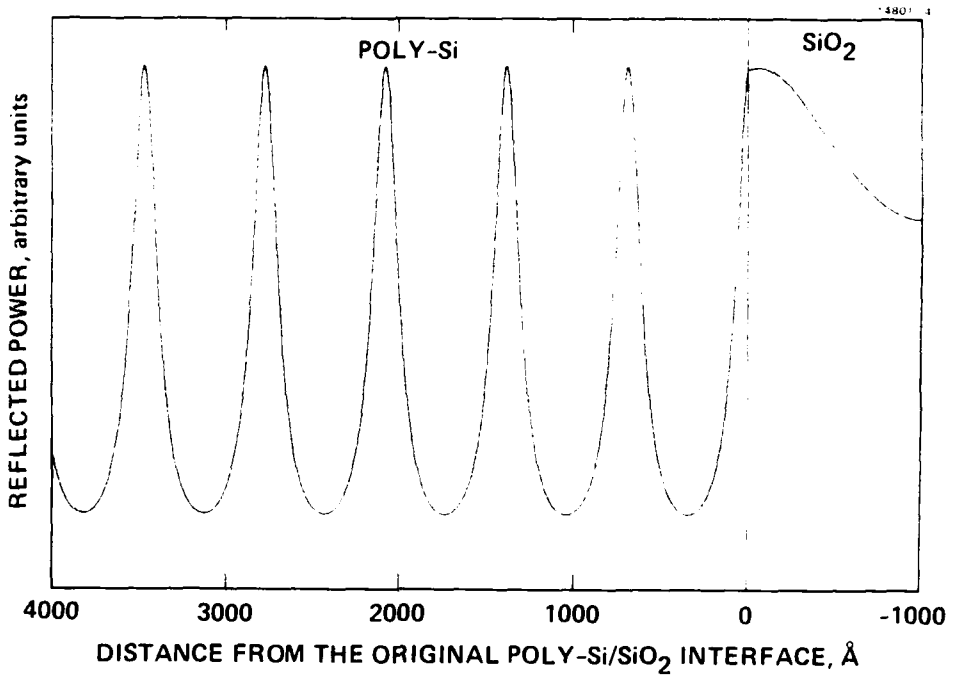

Figure 10. Computer simulation of TRR for poly-Si on SiO_2 on Si. This pattern is for 4000 Å of poly Si over 1000 Å of SiO_2 over Si.

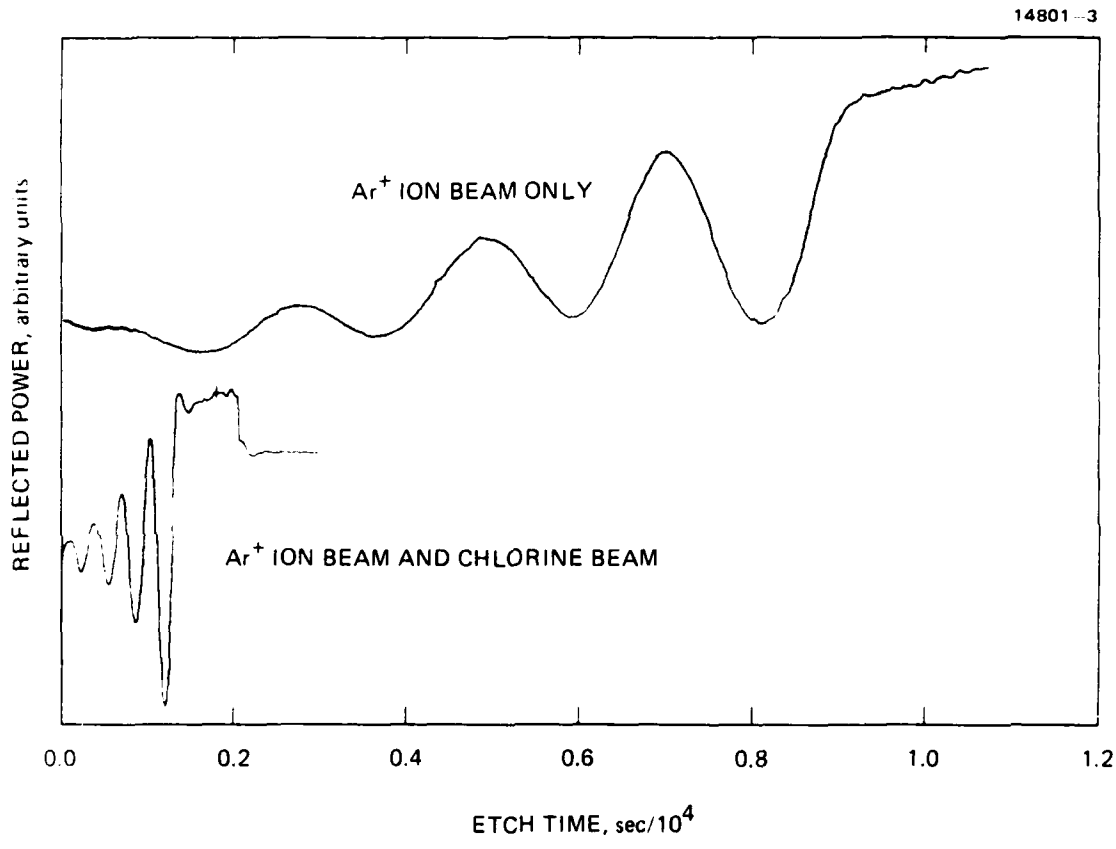

Figure 11. Experimental TRR data for the etching of Poly-Si on SiO_2 on Si. Again, addition of the chlorine beam increases the rate by a factor of 6 over the ion milling rate. With chlorine, the etch rate of poly Si is about three times that of SiO_2.

energy distribution in the beam. One often sees such data obtained by measuring the ion current to the sample during etching as sketched in Figure 12. This is an ambiguous procedure. Not only does it fail to account for production of secondary electrons at the sample, it also overlooks the fact that the ion beam from a Kaufman source is neutralized and thus is a mixture of ions and electrons.[7] (In fact, these beams are neutralized by background electrons even if the neutralizer is intentionally not operated.[13]) We demonstrate the problem by replacing the sample in Figure 12 with a stainless steel sheet and measuring the current to it versus bias voltage while the ion beam is operating (no chlorine). Typical results are shown in Figure 13. The current does not saturate as positive bias increases, which shows that we are collecting the neutralizing electrons with the beam. Quantitative measurements require that the sample be substituted by a current probe which can reject background electrons and suppress secondary electrons at the collector.

Toward this end we have constructed a four-grid retarding field analyzer (RFA) which is shown schematically in Figure 14. The first grid (G1) is held at a negative voltage $-V_1$ to reject background electrons. The second grid (G2) can be ramped through a positive voltage from 0 up beyond beam voltage to retard the beam. The third grid (G3) is held at earth potential for field termination. The fourth grid (G4) is held at a negative voltage $-V_4$ to re-accelerate the ions after energy analysis and to suppress the loss of secondary electrons when the analyzed ions strike the collector plate. The collector is connected to an electrometer at earth potential. A typical retardation profile for a beam at 1 keV is shown in Figure 15.

If the second grid is held at earth potential, the RFA assembly then functions essentially as a Faraday cup and measures total ion beam current free of ambiguities from background and secondary electrons. We have used the RFA in this mode to identify operating conditions of the source which enable a systematic variation of ion current density at the sample. In the course of this work, we discovered that varying the current with beam

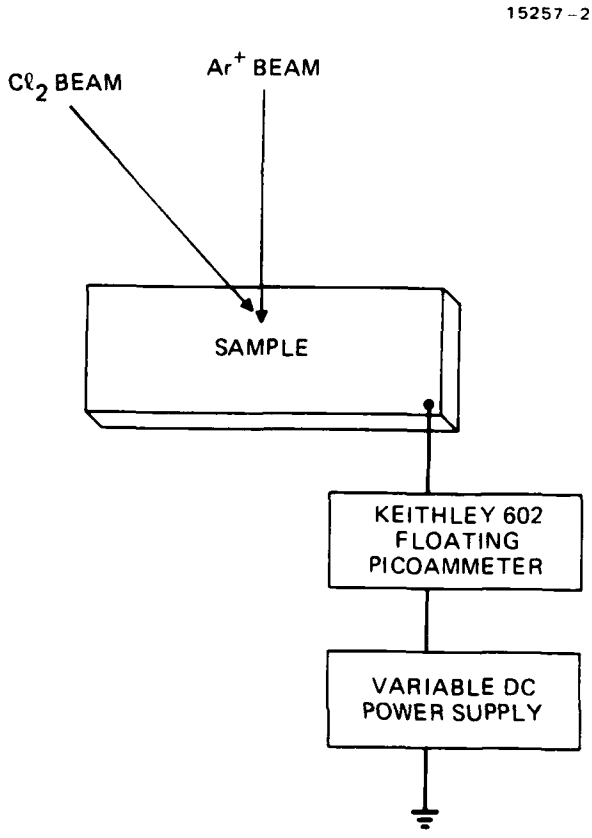

Figure 12. Sample current measurements during etching.

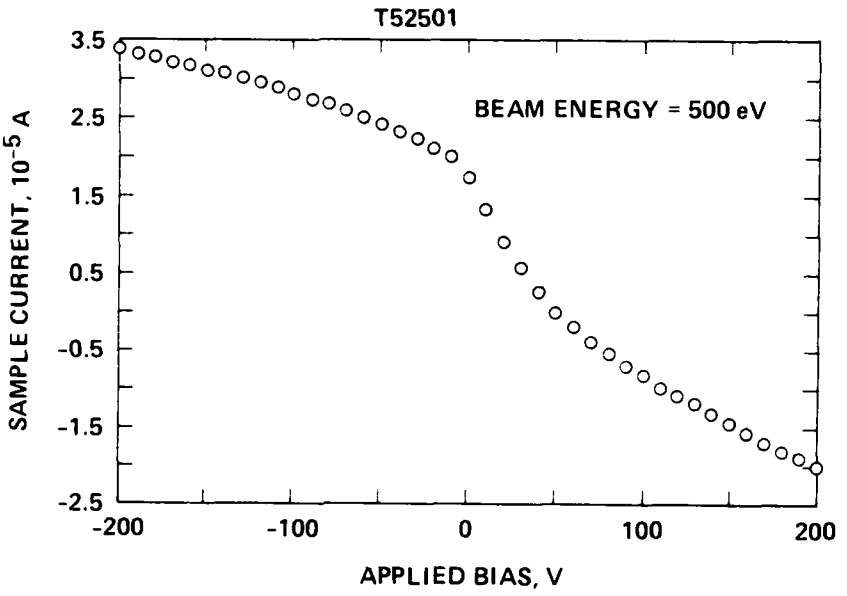

Figure 13. Measurement of ion current to biased probe. The sample has been replaced with a metal sheet. The chlorine beam is not used.

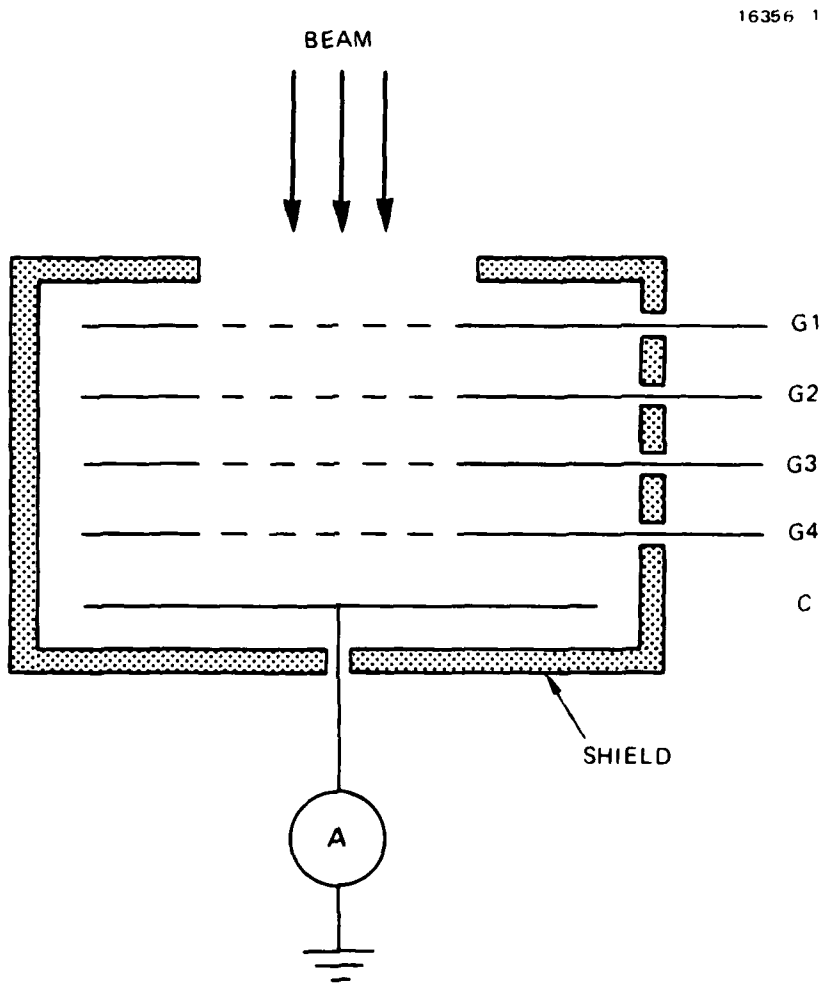

Figure 14. Schematic Retarding Field Analyzer (RFA).

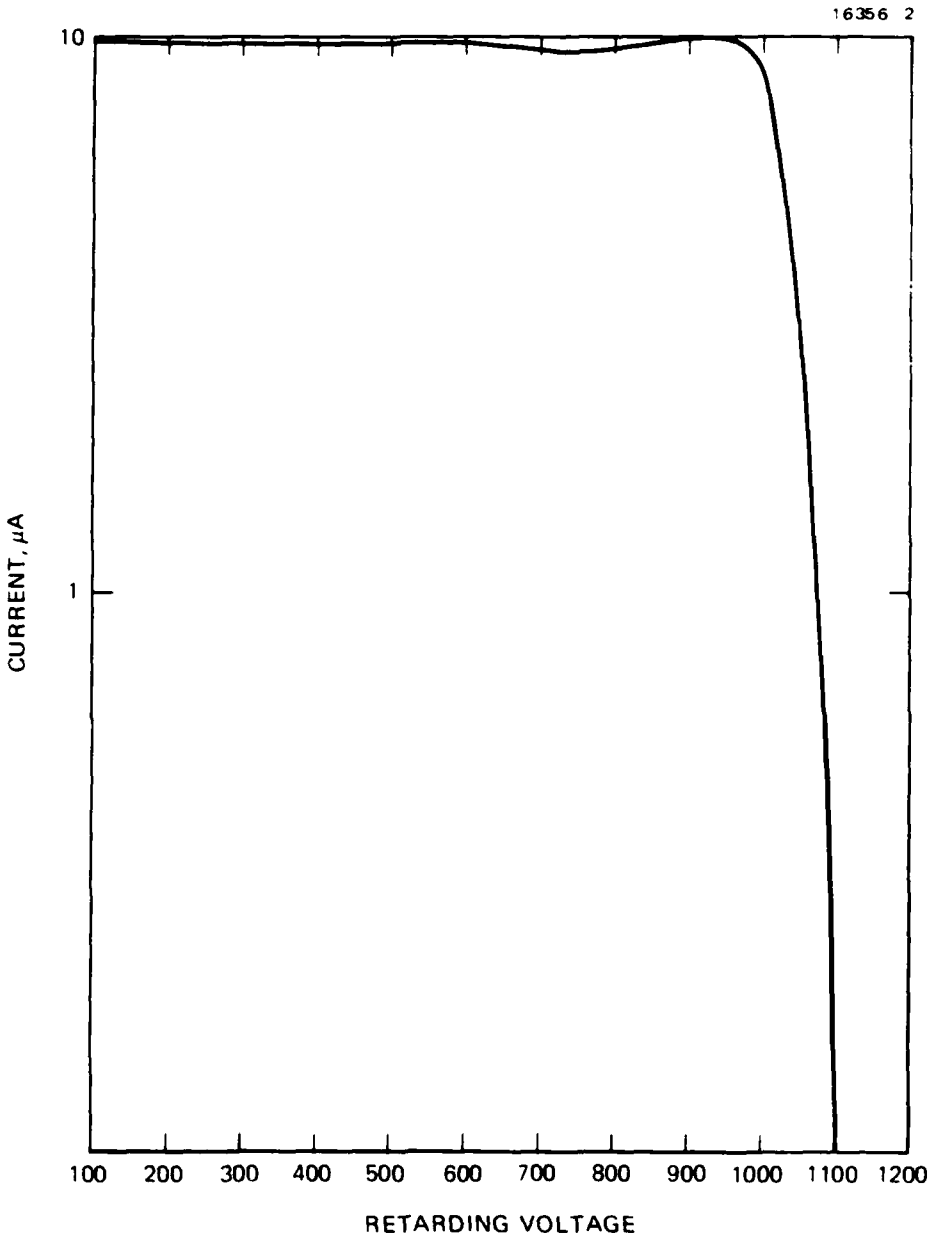

Figure 15. Profile of 1 keV ion beam analyzed by RFA.

energy fixed in a two-grid Kaufman source must be approached with some care. It is known that the screen grid determines the beam energy, while the voltage on the accelerator grid determines not only the total current extracted, but also the spread of the individual beamlets.[7] Usually current is varied by changing the accelerator voltage. We tested the shape and uniformity of the beam by imaging the beam with a phosphor detector similar to those used in LEED systems. The imaging unit is shown schematically in Figure 16. We found that for a given beam energy the accelerator voltage had to be 10-100 V if a good uniform spot was to be obtained. As the accelerator voltage approached 100 V, the spot became very non-uniform and eventually broke into an image of the multi-apertured grids in the source. We have documented these dynamic phenomena on videotape. A sketch of the two extremes of behavior is shown in Figure 17. Once beam energy and accelerator voltage had been set for uniformity, current density could be varied by changing plasma density in the source. The beam spot maintained its uniformity. We measured the current distribution at each plasma density by using the RFA in Faraday mode. We have used these methods to measure the current density in uniform spots produced by 15 sets of beam parameters with energy 500 to 1500 eV. Selected examples are listed in Table 1. We have also included in Table 1 values of current measured (as in Figure 12) while etching samples of a-Si over Si under each set of ion beam conditions. This demonstrates clearly the need for measuring properties of the ion beam by substitution.

Aside from the demonstration of the need for measurement by substitution, our results are significant in two ways. First, the imaging device provides a very quick and simple check on the uniformity of the ion beam. This should be of considerable utility in the processing community where Kaufman sources are popular because they can cover large-area samples. Second, we have shown that the two-grid Kaufman source has very small current density at beam energy below 500 eV. Thus, for low-energy applications a three-grid Kaufman source[7] or some other technology must be used. We will describe these methods and results in detail in a forthcoming publication.

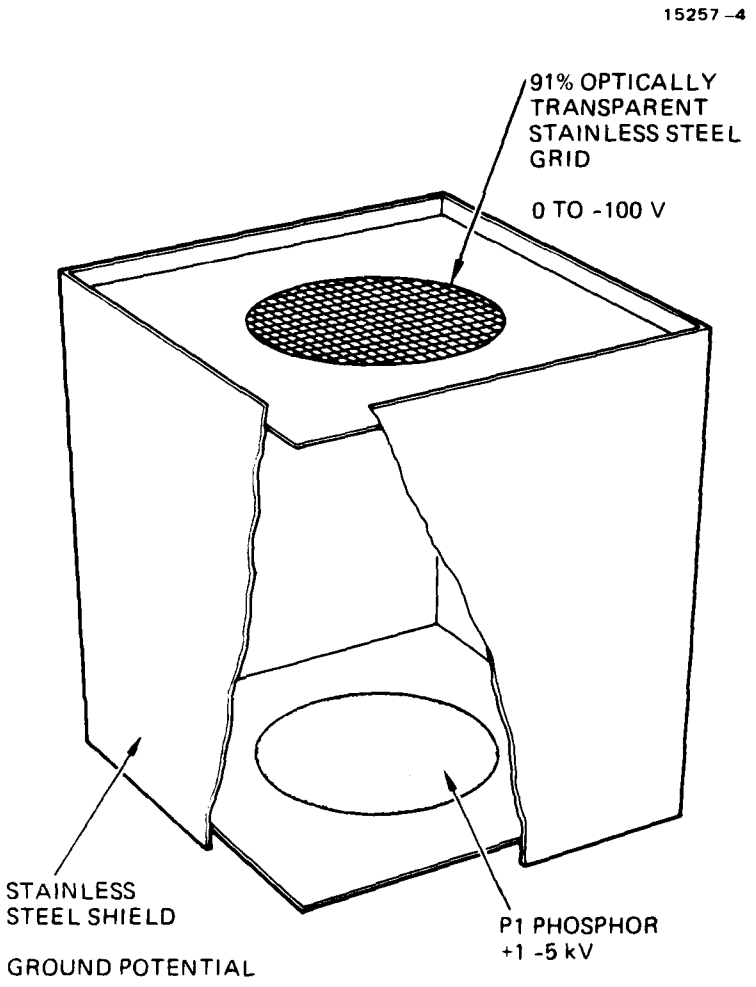

Figure 16. Ion beam imaging unit. Secondary electrons are produced by the beam at the grid and then accelerated to the phosphor to create the image. The bias on the phosphor is always greater than beam energy to prevent sputtering.

15665 1

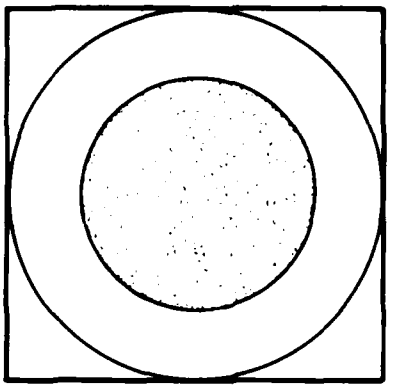

UNIFORM SPOT AT V_{ACC}

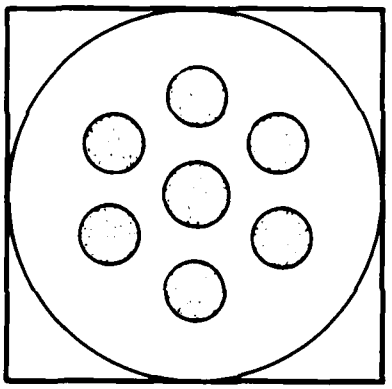

IMAGE OF ACCELERATOR AT HIGH V_{ACC}

Figure 17. Beam image for Kaufman source. For given beam energy, a uniform spot is produced at low V_{acc}; the accelerator grid (with seven apertures) is imaged at high V_{acc}.

Table 1. Characterization of Kaufman Source.

V_{BEAM}	V_{ACC}	I_{DIS} (A)	I_{BEAM} (μA)	Sample Current (μA)
1500	45	0.80	47	87
1500	45	0.60	31	76
1500	45	0.50	18	48
1000	25	0.80	10	32
1000	25	0.60	7	25
1000	25	0.20	4	17
500	25	0.20	2	9
500	25	0.60	1	8

C. KINETIC MEASUREMENTS

In this paragraph we describe measurements of the effect of ion beam energy and flux on the etch rate. All samples were identical: 3600 Å of a-Si over Si, prepared by Si^+ implantation. The ion beam (Ar^+ only) was incident from the normal direction. The Cl_2 flux, calculated to be $2x10^{16}$ molecules $\cdot cm^{-2} \cdot s^{-1}$, was not varied in these experiments. Doubling the flux in preliminary experiments produced no real change in rate, which suggests that this flux is sufficient for saturation coverage. All experiments were done at room temperature. The etch rate was measured by TRR.

In Figure 18, we show rate versus ion flux for several different plasma density values at 500 eV and 1 keV. Ion flux values were calculated from measured current and spot size, assuming the current contained only Ar^+. (This is justified. The source was always operated with its discharge voltage below 40 V; this is known to minimize production of doubly ionized argon.[7]) The results separate into two families, with beam energy as identifying parameter. Within each family the rate is linear with flux, but the slope is different in the two families. This shows that both ion energy and flux are independent variables influencing the etch rate.

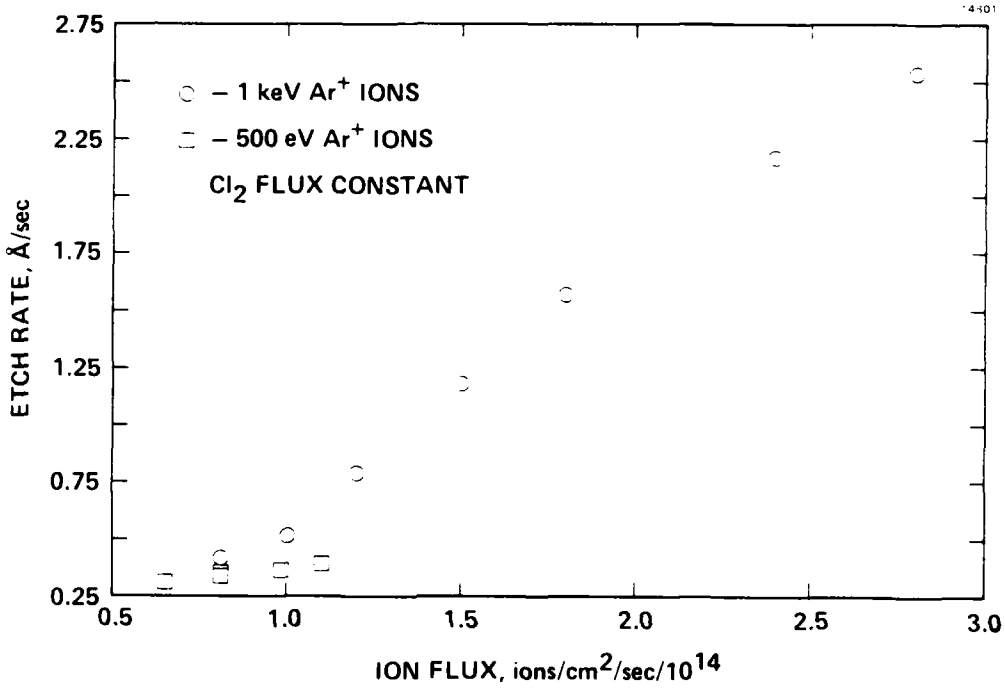

Figure 18. Etching of a-Si on Si substrates as function of Ar^+ ion flux.

The search for a composite single variable which would describe the effect of the ion beam on etching chemistry can be motivated as follows. Since the ion beam is incident from the normal direction, the ion-surface interactions here will resemble implantation more than sputtering. It is plausible that the ion beam stimulates the etching chemistry by creation of damage sites at which the attachment and reaction of the etchant gas are facilitated. According to the theory of radiation damage, the depth of the damaged layer depends on the ion energy and the density of defect sites created depends on the current density.[14] Thus, the volume of the activated or stimulated layer should depend on the *energy flux* of the ion beam. In Figure 19, we plot the same rate data as in Figure 18 versus energy flux, calculated by multiplying ion flux by beam energy. In this form, the two families of rate data appear to coalesce into one. This suggests that energy flux may indeed be a realistic variable. Further, the creation of defects by radiation is an activated process, with an exponential rate law similar to that of chemical reactions.[14] In Figure 20, we replot the data of Figure 19 in Arrhenius form. The results appear to be two different slopes or "activation energies." This suggests that mechanism of the ion-assisted etching reaction might well involve the step of defect creation by the ion beam.

We emphasize that these results are very preliminary and very qualitative. To test these ideas quantitatively will require careful work with a mass-analyzed low energy ion beam having a narrow energy distribution (perhaps monochromatized by an energy analyzer) and a well-characterized current density. Such experiments should be done because energy flux is an attractively simple property of the ion beam, and as seen above provides a conceptually smooth way to include effects of the ion beam on etching chemistry. It is, therefore, an attractive ingredient for tailoring practical processes. Moreover, a generalized theory of radiation damage coupled to chemical reaction with adsorbed vapors should be feasible.

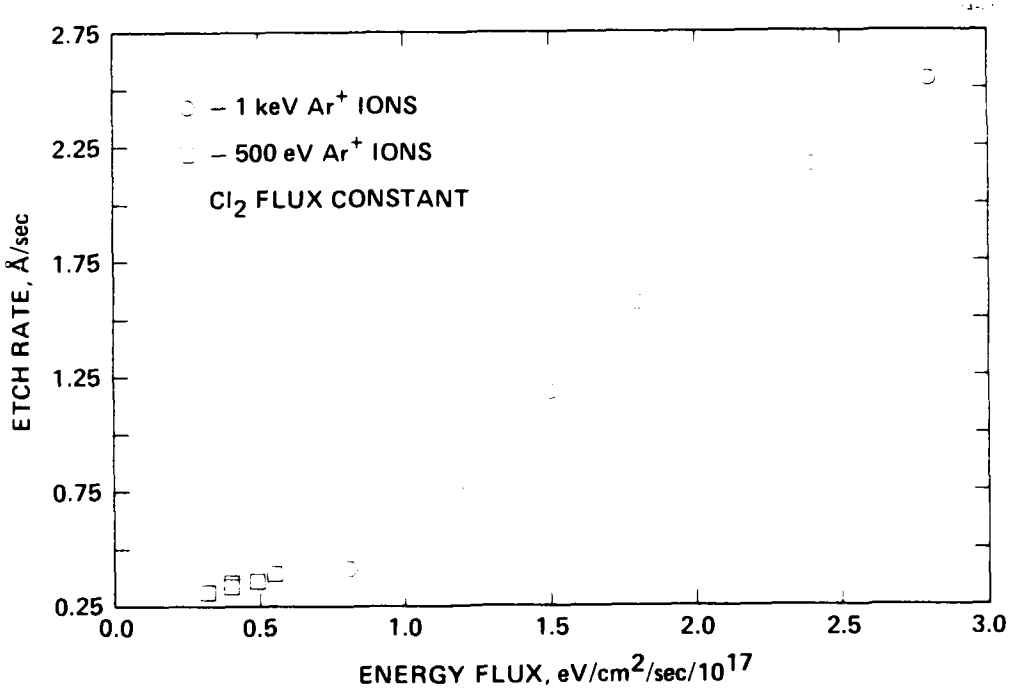

Figure 19. Etching of a-Si on Si substrates as a function of ion beam energy flux.

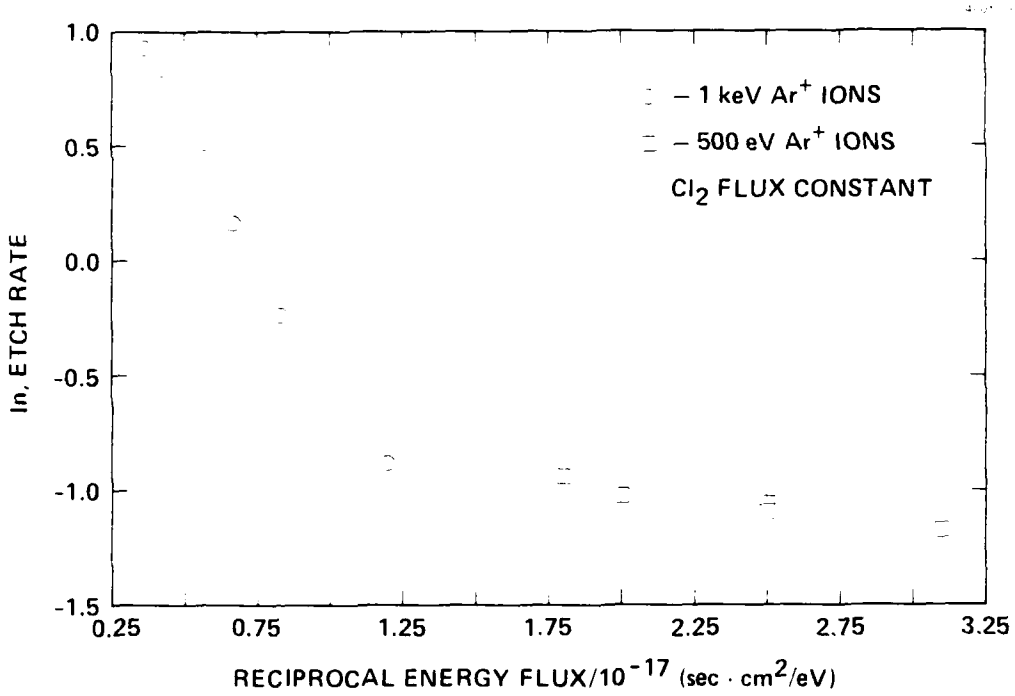

Figure 20. Arrhenius plot of the a-Si etch rate versus reciprocal ion energy flux.

D. MASS SPECTROMETRY RESULTS

Monitoring the reactions by MS, we found $SiCl_x^+$(x=1,2,3,4) in the spectra from both Si and SiO_2. A typical spectrum is shown in Figure 21. Peak heights were always in order $SiCl^+ > SiCl_2^+ > SiCl_3^+ > SiCl_4^+$. This suggests that the corresponding neutral fragments depart the target as primary products and are not produced solely by fragmentation of $SiCl_4$ in the MS ionizer, since the cracking pattern of $SiCl_4$ shows much larger peaks for $SiCl_3^+$ and $SiCl_4^+$.[9d] There have been other reports on IBAE of Si by Cl_2, with some disagreement on whether the primary neutral products are $SiCl_4$ or the less chlorinated fragments.[9] This is probably because in all systems involved, Cl_2 is delivered by a small tube without differential pumping; thus the reactive flux is not well controlled and varies substantially among systems. Definitive identification of the primary products is best accomplished by timing experiments with a modulated molecular beam. We are at present preparing to make these measurements. Pending the outcome of these experiments, we selected $SiCl^+$ for continuous monitoring through layered samples of Si and SiO_2.

We have obtained experimental data for layered samples as simultaneous traces of TRR patterns and ion current. One example shown in Figure 22 is for a sample comprising 4000 Å polysilicon over 1000 Å SiO_2 over bulk Si etched with Ar^+ ions (1keV; 8×10^{13} ions$\cdot cm^{-2} \cdot s^{-1}$) and Cl_2 as above. By comparing the TRR pattern to the computer-generated standard in Figure 10 for this material, we found that the polysilicon etched only three times as fast as the oxide under these conditions. In a sequence of samples run at different ion energies but all other conditions fixed, selectivity improved as the beam energy was lowered and worsened as it was increased. A qualitative indication of the mechanism behind these relative rates is given by the MS trace, where the $SiCl^+$ falls as the etch goes from poly Si into the oxide layer, then increases again upon passage from the oxide to the bulk Si. As the ion beam energy was reduced, the fall in $SiCl^+$ at the poly Si/SiO_2 interface increased, suggesting that the ion-enhanced

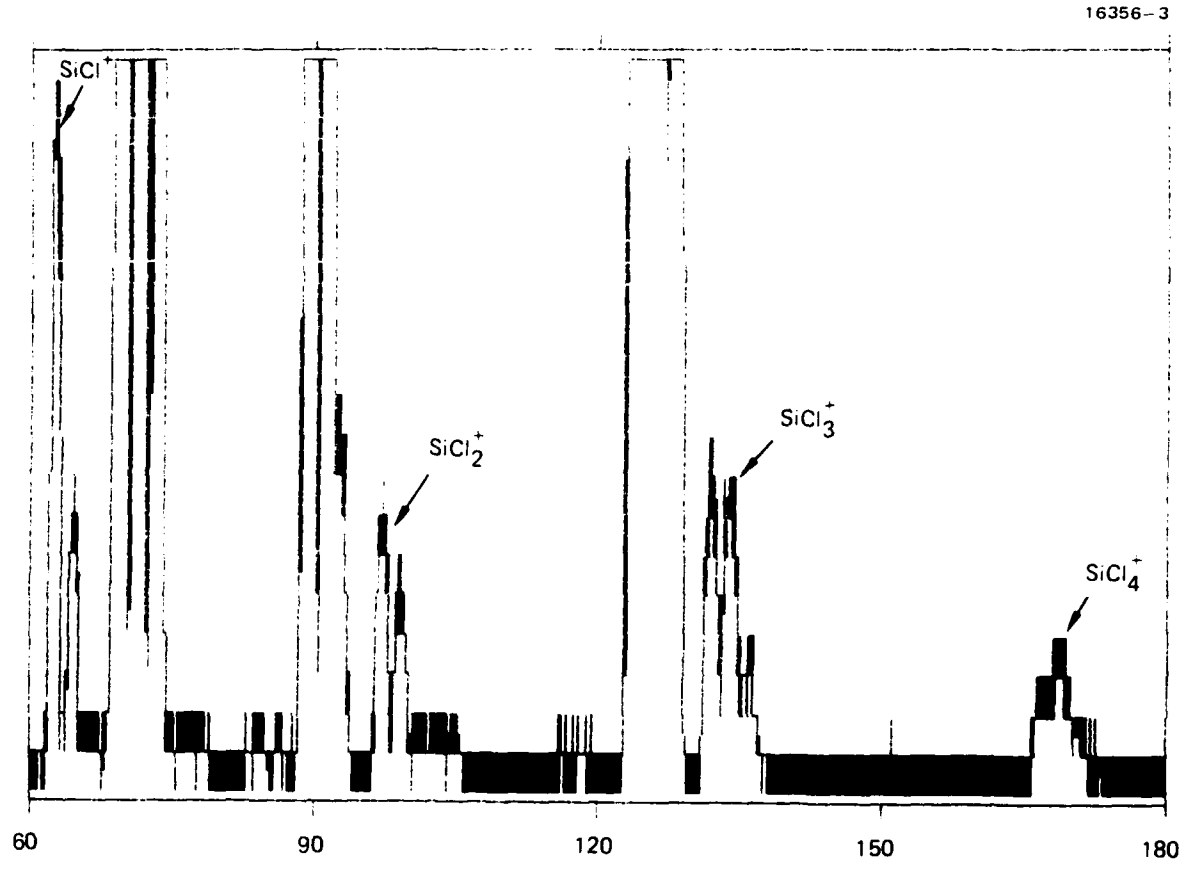

Figure 21. Mass spectrum of etch products from Si with Ar^+ and Cl_2 beams. $SiCl^+$ is at 63 amu, $SiCl_2^+$ at 98, $SiCl_3^+$ at 133, $SiCl_4^+$ at 168. This spectrum was acquired without the chopper and shows a background of chlorine.

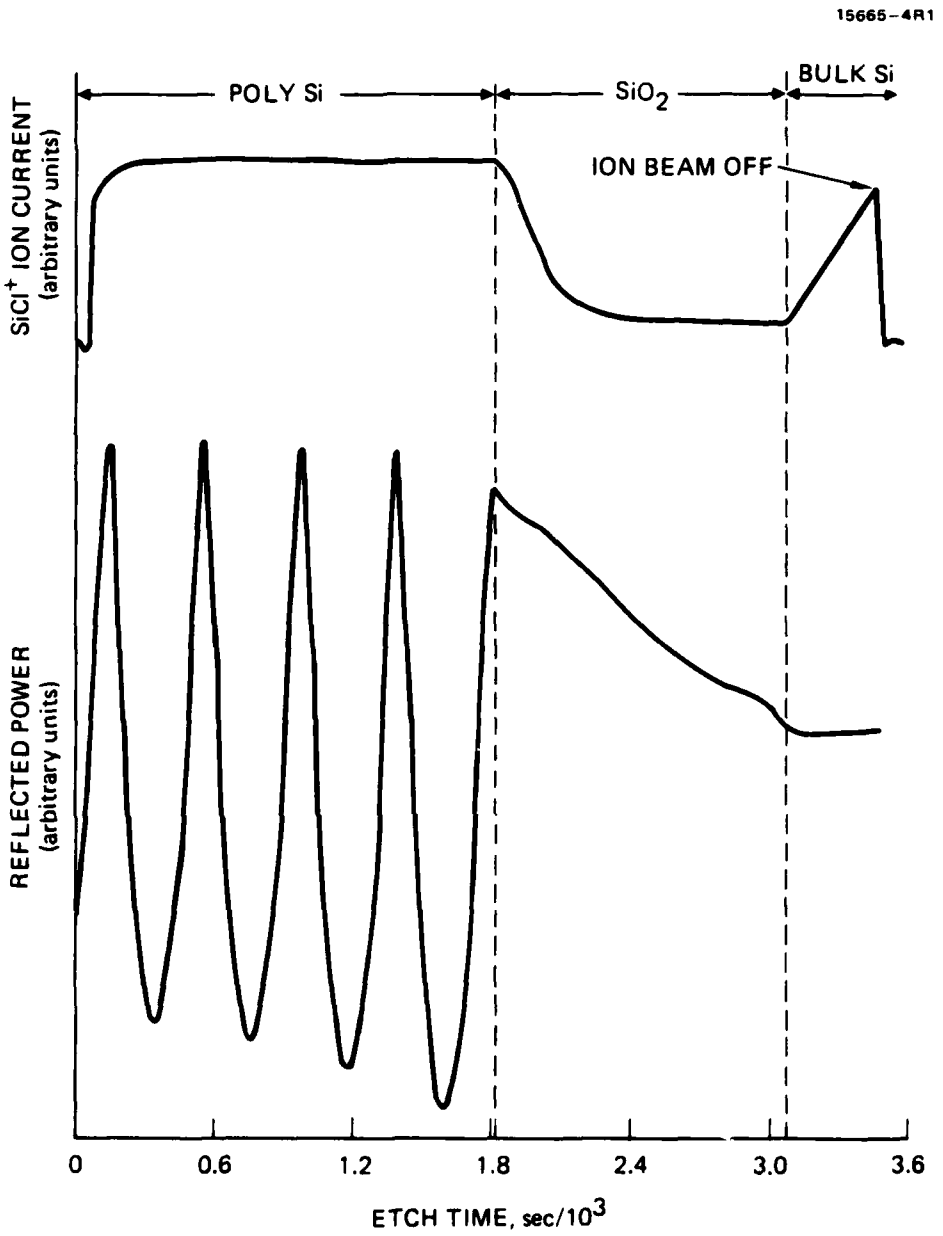

Figure 22. Simultaneous TRR and MS data for poly Si/SiO_2 in IBAE.

chemical reaction rate for polysilicon relative to SiO_2 depends strongly on ion energy. In order to make this mechanistic interpretation quantitative and to learn how the ion beam influences the relative etch rate, it will be necessary to identity the primary products with certainty and record each simultaneously with the TRR signal. We are at present placing the simultaneous acquisition of TRR and MS data under computer control so that several products can be followed simultaneously. In this way we will obtain a "depth profile" of the reactivity of layered samples using TRR as the depth index.

E. REACTION MODEL FOR SELECTIVITY

Our results can be synthesized into a reaction model based on the implantation-damage ideas introduced in Section 2C above. The model is summarized in Figure 23. The ion beam, incident from the normal direction, creates a damaged layer whose thickness depends upon the ion energy. The chlorine arrives at the surface and undergoes ion-enhanced diffusion[15] into the damaged layer and reacts with the silicon to form volatile products which migrate to the surface and desorb. Thus at steady state the ion-assisted etching process is a complicated mix of reaction and transport process in which the damage front and the diffusion front advance into the film. If the ion energy is too great, the damage front leads the reaction front by too great a distance and moves on into the oxide layer where it breaks Si-O bonds. This causes chemical reduction of the oxide and destroys the inherent selectivity between it and the polysilicon. Thus the key to good selectivity would be to keep the ion beam energy low enough to have only very shallow damage layers and to minimize rupture of Si-O bonds.

Independent confirming evidence for such a model is difficult to obtain. Our own attempts to determine the depth distribution of Ar and Cl in such samples, interrupted at various stages of etching, by AES and XPS depth profiling (Ne^+ sputter beam) have been inconclusive, perhaps because samples are exposed to air

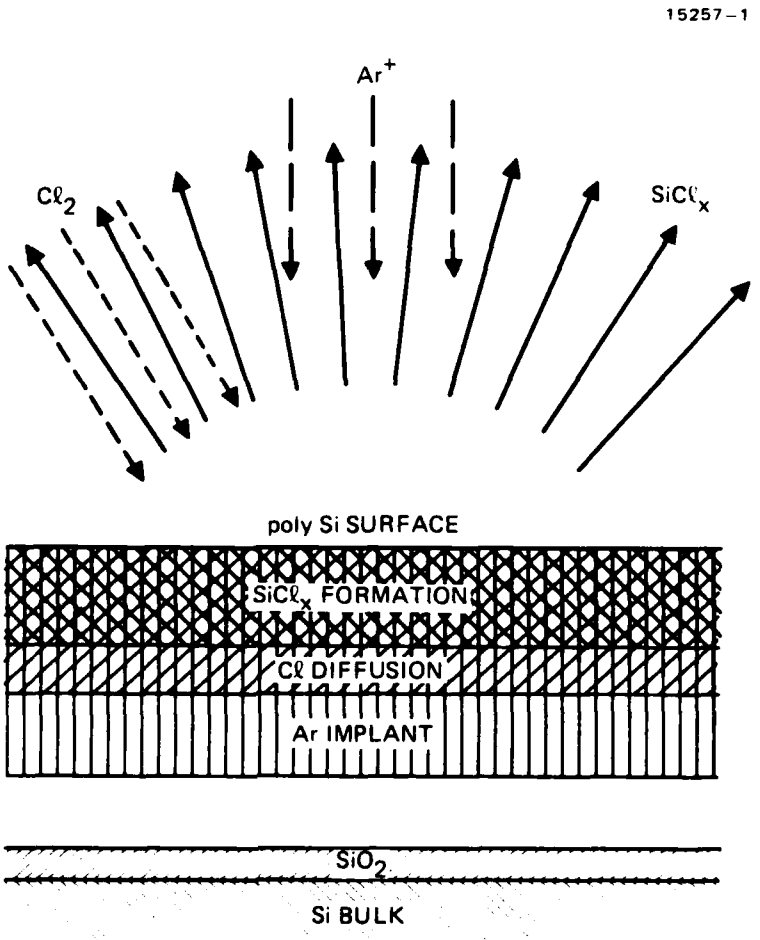

Figure 23. Implantation-diffusion model of ion-assisted etching.

between etching and analysis. Mayer and his collaborators have used Rutherford back-scattering techniques to demonstrate that low energy ion beams in the etching configuration do cause a shallow damage layer.[16]

F. RESULTS FOR PATTERNED SAMPLES

In this paragraph we show scanning electron micrographs of the results of etching simple photoresist test patterns into Si substrates by IBAE. These micrographs show the consequences of having both the ions and the reactive species arrive at the pattern as well-defined beams. In all cases shown, the ion beam was Ar^+ at 1 keV and the reactive beam was Cl_2 at about $2x10^{16}$ molecules$\cdot cm^{-2}\cdot s^{-1}$. The Ar^+ and Cl_2 beams were always 45° apart as shown in Figure 3. The samples could be rotated about the polar axis to be normal to either beam. At any polar position, the sample could also be rotated about the azimuthal axis. In each illustration we provide reference directions to help visualize the orientation of the pattern relative to the beams, as well as the direction of the cross section shown. Resists have not been stripped.

In Figure 24, we see a line where Ar^+ was normal and Cl_2 came from the right at 45°. Note that the trench on the right-hand side is deeper than the one on the left. We believe the shallow trench on the left, in an area shielded from Cl_2, is the standard sort of trench seen in ion beam milling from the normal direction, caused by ions reflected from the sidewall onto the substrate. We believe the deeper trench on the right is caused by an increased local concentration of Cl_2 due to reflection from the mask. In this corner, the IBAE rate is increased because the local concentration of both ionic and reactive fluxes is increased by reflection. On the left side note the plateau which was shielded from Cl_2, as well as the smooth ramp which saw Cl_2 directed at 45° and in regular concentration unaffected by shadowing. In Figure 25, we show the same pattern etched in the same configuration but sectioned and viewed in the other direction. This time the Cl_2 entered parallel to the mask lines

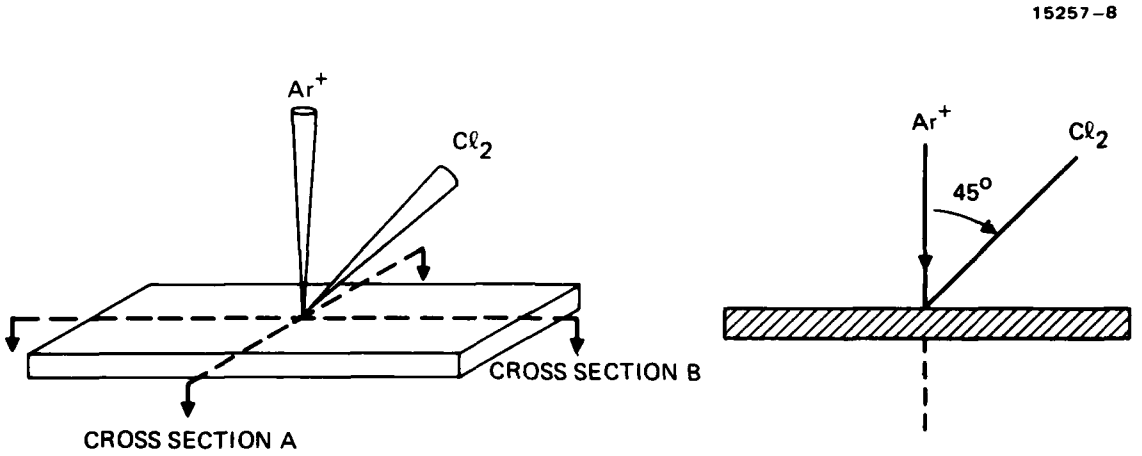

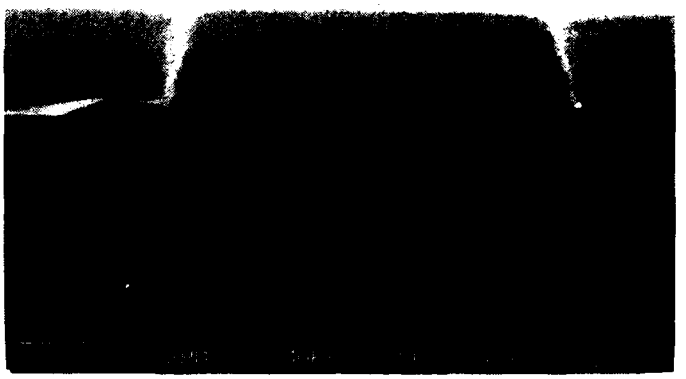

CROSS SECTION B

Figure 24. Etching photoresist test patterns into Si substrates. Sample is normal to ion beam, and the chlorine beam is shadowed.

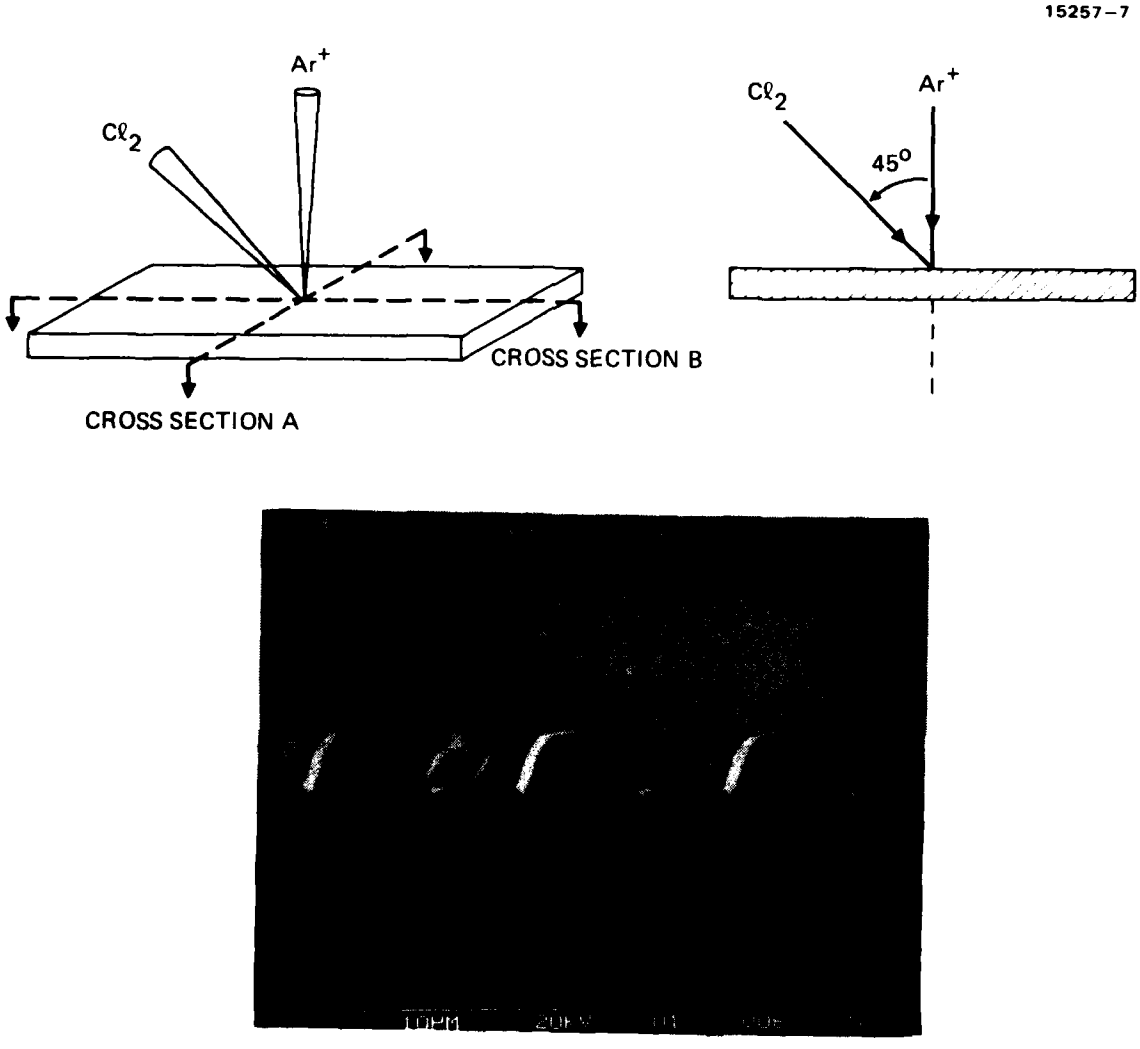

Figure 25. Etching photoresist test patterns into Si substrates. Sample is normal to ion beam, and neither beam is shadowed.

direction. This time the Cl_2 entered parallel to the mask lines (but still 45° below normal in the polar direction) so that there was no shadowing, i.e., the sample was rotated 90° in the azimuthal plane. The features are quite symmetrical. Both corners can receive reflected ions, and both receive Cl_2 flowing along the pattern lines, so the "enhanced" trenches appear. In Figure 26, we show the results of having the Cl_2 normal to the sample and the ion beam shadowed by the features. Note the interesting effects. In Figure 27, we show the consequences of moving the sample 90° in the azimuthal plane so that the ion beam is not shadowed.

In all our work on patterned samples we have seen very smooth and clean surfaces with no evidence of "grass" or re-deposition. We attribute this to the fact that we have a very clean vacuum system and that we do not have a plasma interacting with the walls of the chamber. We have seen that the patterned effects are clearly attributable to the superposition of beams arriving at the substrate through whatever combination of masks and shadows. This suggests that for deep openings with vertical walls the beams should be nearly co-linear. In addition, the ion beam energy should be reduced so that ions reflected from the sidewall no longer have sufficient energy to cause trenching at the substrate. Figures 24 and 26 demonstrate the exciting prospect that specifically sloped walls and controlled undercut can be obtained by proper combinations of beam flux and geometry.

Figure 26. Etching photoresist test patterns into Si substrates. Sample is normal to chlorine beam, and ion beam is shadowed.

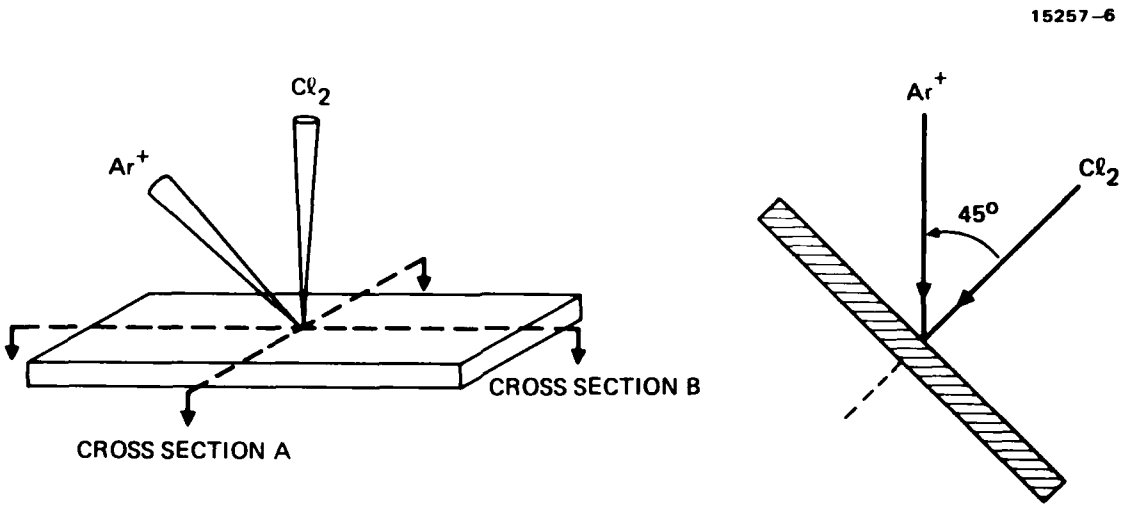

CROSS SECTION A

Figure 27. Etching photoresist test patterns into Si substrates. Sample is normal to chlorine beam, and neither beam is shadowed.

SECTION 3

DISCUSSION OF RESULTS

We undertook this program not to examine reaction dynamics in molecular detail, but rather to explore middle ground between reaction fundamentals and processing applications. Our objective was to identify those fundamental issues which need to be addressed so that practical beam etching processes can be designed in a rational way. We devoted considerable attention to the role of transport processes in the reactions, since the kinetics of heterogeneous surface reactions are always coupled with, and complicated by, transport effects.[17] We saw that the results on patterned samples are geometrical superpositions of the directed transport of ions and of reactive molecules to the substrate. We saw no isotropic etching, which we attribute to the absence of reactive species diffusing to the sample from random directions. We saw undercutting only when we intentionally directed both beams onto sidewalls. The geometrical results produced can be combinations of anisotropic etching, trenching, and shadowing. We obtained rate data which suggest that the question of selectivity in layered samples depends on the transport of kinetic energy into and through the reacting layer. Our findings have some implications for the design of practical beam processing systems and for directions of subsequent research. We offer some comments in these areas.

A. APPLICABILITY

One very useful feature of IBAE of silicon and SiO_2 with Cl_2 is the fact that the reaction only takes place where it is stimulated by the ion beam. This coupled with the fact that the reaction rate saturates as Cl_2 coverage increases[18] and with our demonstration of shadowing effects suggest that a practical system design should emphasize geometry more than flux (so long as flux is sufficient) when placing the reactive beam. For etching narrow features with high aspect ratios, the reactive beam

should be nearly co-linear with the normally incident ion beam. For etching special tapered walls and controlled under-cutting, the beams should have directional separation.

For high-resolution etching of very fine features, it may be desirable to have both species come from the same source, even though independent control of the species must be sacrificed. This can be achieved in Reactive Ion Beam Etching (RIBE), where the plasma ion source is operated on reactive gases. Early attempts at RIBE in this country[19] produced good patterns by operating hot-filament Kaufman sources on gases like Freon or Cl_2, but faced problems of low rate, inadequate selectivity, and short filament lifetime. It was perhaps not always appreciated that a large part of the rate depended on the effusion of neutral reactive fragments from source to substrate and, therefore, on system geometry. Moreover, the restrictions of Kaufman sources to fairly high energy ions, seen here to have a deleterious effect on selectivity, still apply to reactive ions.

Considerable advances have been made on RIBE in Japan, both for silicon and III-V technology.[20] In place of Kaufman sources, these systems have relied upon Electron Cyclotron Resonance (ECR) plasmas produced by microwaves at 2.45 GHz and a magnetic field. These ECR sources have long lifetime with reactive gases. Special ion extraction systems, sometimes relying only on magnetic fields, produce ion beams at energy below 100 eV. The importance of ultrahigh vacuum and of *in situ* surface analysis has been recognized in these systems.[21]

B. COMPARISON WITH OTHER PROGRAMS

Ion-stimulated surface chemistry has become a very active field of research. There are programs at North Carolina,[16,22] Cornell,[23] MIT,[9b] Berkeley,[24] Lincoln Laboratories,[25] Bell Laboratories,[9c] Philips Laboratories,[9d,26] and Hughes Research Laboratories, as well as the pioneering program at IBM San Jose.[2,3] There is a very interesting development of IBAE in Japan in which maskless etching is accomplished by application of

a focused ion beam in a reactive ambient.[27] In general, the academic programs address quite fundamental issues of detailed molecular mechanisms. There is both fundamental and applied work in the industrial programs, with some emphasis on empirical process development. Our program has been intermediate, identifying the fundamental problem in one specific area of applications. So far as we are aware, ours is the only program emphasizing direct studies of selectivity on real layered samples. We believe our use of TRR and MS to study the effects of beam conditions on the reactivity of layered samples as function of a depth is unique.

C. RECOMMENDATIONS

We have shown that ion beam enhanced etching (IBAE) is a promising approach for layered samples and that TRR and MS simultaneously are useful *in situ* probes for studying selectivity. We have identified low selectivity as the main impediment to practical implementation of IBAE, and we have traced this to the inability of our present ion sources to operate at low energy. We suggest that subsequent work in IBAE emphasize the practical aspects of producing intense ion beams at energy 50-500 eV and the fundamental mechanisms of interaction between low energy ions and surfaces.

REPORTS AND PUBLICATIONS

Semi-annual reports were submitted throughout the program.

Two papers based on work performed in the program were presented at conferences:

1. H.P. Gillis and W.J. Gignac, "Ion-enhanced etching of Si and SiO_2 by Cl_2," presented at the 32nd National Symposium of American Vacuum Society, Houston, TX, Nov. 1985. To be published in J. Vac. Sci. Tech., May-June 1986.

2. H.P. Gillis and W.J. Gignac, "Ion-enhanced etching for CMOS applications," presented at the 1985 Fall Meeting of the Materials Research Society, Boston, MA, Dec. 1985.

PERSONNEL

The following Hughes Research Laboratories personnel participated in this program.

H.P. Gillis, Ph.D., Member of the Technical Staff.

W.J. Gignac, Ph.D., Member of the Technical Staff.

A.R. Ward, Technical Support.

C.P. Hoberg (deceased), Technical Support.

No academic degrees were based on this work.

REFERENCES

1. R.A. Morgan, Plasma Etching in Semiconductor Fabrication, Elsevier, New York, 1985.

2. J.W. Coburn and H. Winters, J. Appl. Phys. 50, 3189 (1979).

3. (a) H.F. Winters, JVST B3, 9 (1985); (b) H.F. Winters and J. Coburn, JVST B3, 1376 (1985).

4. (a) W.D. Davis and T.A. Vanderslice, Phys. Rev. 131, 219 (1963); (b) J.W. Coburn, Rev. Sci. Instr. 41, 1219 (1970).

5. (a) S.W. Pang, D.D. Rathman, D.J. Silverman, R.W. Mountain, and P.D. DeGraff, J. Appl. Phys. 54, 3272 (1983); (b) S.W. Pang, M.W. Geis, N.N. Efremow, and G.A. Lincoln, JVST B3, 398 (1985).

6. C.G. Tuppen, R. Heckingbottom, M. Gill, C. Heslop, and G.J. Davies, Surf. Interface Anal., 6, 267 (1984).

7. H.R. Kaufman, J.J. Cuomo, and J.M.E. Harper, JVST 21, 725 (1982).

8. C.B. Lucas, Vacuum 23, 395 (1972).

9. (a) H.F. Winters and F.A. Houle, J. Appl. Phys. 54, 1218 (1983); (b) R.A. Rossen and H.H. Sawin, Appl. Phys. Lett. 45, 860 (1984); (c) S.C. McNevin and G.E. Becker, JVST B3, 485 (1985); (d) A.W. Kolfschoten, R.A. Haring, A. Haring, and A.E. de Vries, J. Appl. Phys. 55, 3813 (1984).

10. (a) G.L. Olson, S.A. Kokorowski, R.A. McFarlane, and L.D. Hess, Appl. Phys. Lett. 37, 1019 (1981); (b) G.L. Olson, S.A. Kokorowski, J.A. Roth, R.S. Turley, and L.D. Hess, Proc. SPIE 276, 128 (1981).

11. (a) P.J. Marcoux and P.-D. Foo, Proc. SPIE 276, 170 (1981); (b) H.H. Busta, R.E. Lajos, and D.A. Kiewit, Sol. St. Technol., February 1979, 61-64.

12. P.A. Heimann and R.J. Schutz, J. Electrochem. Soc. 131, 881 (1984).

13. D.B. Langmuir, E. Stuhlinger, and J.M. Sellen, Jr., (eds.), Electrostatic Propulsion, Academic Press, New York, 1961. (Volume 5 in the series Prog. Astronautics and Rocketry)

14. G. Carter and J.S. Colligon, Ion Bombardment of Solids, Elsevier, New York, 1973. Chapter 6.

15. (a) A. Zomorrodian, S. Tougaard, and A. Ignatiev, JVST A1, 339, (1983); (b) W. Wach and K. Wittmaack, J. Appl. Phys. 52, 3341 (1981); (c) R. Miranda and J.M. Rojo, Vacuum 34, 1069 (1984).

16. D.J. Vitkavage, C.J. Dale, W.K. Chu, T.G. Finstad, and T.M. Mayer, Nucl. Instr. Meth. B13, 313 (1986).

17. S.T. Ceyer and G.A. Somorjai, An. Rev. Phys. Chem. 28, 477 (1977).

18. U. Gerlach-Meyer, J.W. Coburn, and E. Kay, Surf. Sci. 103, 177 (1981).

19. (a) D.M. Brown, B.A. Heath, T. Coutumas, and G.R. Thompson, Appl. Phys. Lett. 37, 159 (1980); (b) J.M.E. Harper, J.J. Cuomo, P.A. Leary, G.M. Summa, H.R. Kaufman, and F.J. Bresnock, J. Electrochem. Soc. 128, 1077 (1981); (d) T.M. Mayer, R.A. Barker, and L.J. Whitman, JVST 18, 349 (1981).

20. (a) S. Matsuo and Y. Adachi, Japan. Jour. Appl. Phys. 21, L4 (1982); (b) M. Miyamura, O. Tsukakoshi, and S. Komiya, JVST 20, 986 (1982); (c) K. Asakawa and S. Sugata, JVST B3, 402 (1985); (d) K. Suzuki, K. Ninomiya, and S. Nishimatsu, Vacuum 34, 953 (1984).

21. (a) K. Ninomiya, K. Suzuki, S. Nishimatsu, Y. Gotoh, and O. Okada, JVST B2, 645 (1984); (b) K. Asakawa and S. Sugata, JVST A4, 677 (1986).

22. E.L. Barish, D.J. Vitkavage, and T.M. Mayer, J. Appl. Phys. 57, 1336 (1985).

23. (a) J.D. Chinn and E.D. Wolf, JVST B3, 410 (1985). (b) S. Park, L.C. Rathbun, and T.N. Rhodin, JVST A3 791 (1985).

24. D.R. Olander and M. Balooch, "Thermal and Ion-Assisted Reactions of $Al_{0.3}Ga_{0.7}As$ with Molecular Chlorine," presented at 1986 Spring Meeting of the Materials Research Society, Palo Alto, CA, April 1986.

25. N.L. Demeo, J.P. Donnelly, F.J. O'Donnell, M.W. Geis, and K.J. O'Connor, Nucl. Inst. Meth. B7, 814 (1985) and references therein.

26. J. Dieleman, F.H.M. Sanders, A.W. Kolfschoten, P.C. Zalm, A.E. de Vries, and A. Haring JVST B3, 1384 (1985).

27. Y. Ochiai, K. Gamo, and S. Namba, JVST B3, 67 (1985).

END

10-86

DTIC